



# Combination of RNAseq and RADseq to Identify Physiological and Adaptive Responses to Acidification in the Eastern Oyster (*Crassostrea virginica*)

Caroline Schwaner<sup>1</sup> · Sarah Farhat<sup>1,2</sup> · Isabelle Boutet<sup>3</sup> · Arnaud Tanguy<sup>3</sup> · Michelle Barbosa<sup>1</sup> · Denis Grouzdev<sup>1</sup> · Emmanuelle Pales Espinosa<sup>1</sup> · Bassem Allam<sup>1</sup>

Received: 27 February 2023 / Accepted: 29 September 2023

© The Author(s), under exclusive licence to Springer Science+Business Media, LLC, part of Springer Nature 2023

## Abstract

Ocean acidification (OA) is a major stressor threatening marine calcifiers, including the eastern oyster (*Crassostrea virginica*). In this paper, we provide insight into the molecular mechanisms associated with resilience to OA, with the dual intentions of probing both acclimation and adaptation potential in this species. *C. virginica* were spawned, and larvae were reared in control or acidified conditions immediately after fertilization. RNA samples were collected from larvae and juveniles, and DNA samples were collected from juveniles after undergoing OA-induced mortality and used to contrast gene expression (RNAseq) and SNP (ddRADseq) profiles from animals reared under both conditions. Results showed convergence of evidence from both approaches, particularly in genes involved in biomineralization that displayed significant changes in variant frequencies and gene expression levels among juveniles that survived acidification as compared to controls. Downregulated genes were related to immune processes, supporting previous studies demonstrating a reduction in immunity from exposure to OA. Acclimation to OA via regulation of gene expression might confer short-term resilience to immediate threats; however, the costs may not be sustainable, underscoring the importance of selection of resilient genotypes. Here, we identified SNPs associated with survival under OA conditions, suggesting that this commercially and ecologically important species might have the genetic variation needed for adaptation to future acidification. The identification of genetic features associated with OA resilience is a highly-needed step for the development of marker-assisted selection of oyster stocks for aquaculture and restoration activities.

**Keywords** ddRADseq · RNAseq · Oysters · Ocean acidification · SNPs

## Introduction

Anthropogenic climate change is a considerable stressor for marine organisms. The response of species, populations, and individuals to future climate regimes is not fully

understood. Studies have demonstrated that organisms are able to respond to altered environments through various mechanisms within their lifetimes as well as through evolutionary processes (Calosi et al. 2013; Evans et al. 2013; Reusch 2013; Schluter et al. 2014; Sunday et al. 2014);

✉ Bassem Allam  
bassem.allam@stonybrook.edu

Caroline Schwaner  
caroline.schwaner@stonybrook.edu

Sarah Farhat  
farhat.sarah@gmail.com

Isabelle Boutet  
isabelle.boutet@sb-roscoff.fr

Arnaud Tanguy  
atanguy@sb-roscoff.fr

Michelle Barbosa  
michellebarbosa810@gmail.com

Denis Grouzdev  
denis.grouzdev@stonybrook.edu

Emmanuelle Pales Espinosa  
emmanuelle.palesespinosa@stonybrook.edu

<sup>1</sup> School of Marine and Atmospheric Sciences, Stony Brook University, Stony Brook, NY 11790, USA

<sup>2</sup> Institut Systématique Evolution Biodiversité (ISYEB), Muséum national d'Histoire naturelle, CNRS, Sorbonne Université, EPHE, Université des Antilles, Paris, France

<sup>3</sup> Station Biologique de Roscoff, CNRS/Sorbonne Université, Place Georges Teissier 29680, Roscoff, France

however, investigating the acclimation and adaptation potentials of marine species to ocean acidification (OA) is still in its infancy (Saba et al. 2019).

Shellfish-growing areas, such as shallow estuaries, are often exposed to eutrophication and experience periods of reduced oxygen, variable alkalinity, oscillations in pH, extreme acidification, low salinity, and high temperature (Wallace et al. 2014; Baumann et al. 2015). These changes arise from both natural biogeochemical cycling as well as through sustained anthropogenic disturbances. The eastern oyster (*Crassostrea virginica*) tolerates spatio-temporally variable environments such as those encountered in New York's coastal embayments which already face acute exposure to elevated  $p\text{CO}_2$  and low pH that are greater than predicted climate driven changes (Baumann et al. 2015).

Alterations in carbonate chemistry can induce physiological responses that necessitate alterations in gene expression, and studies have demonstrated that marine organisms can regulate gene expression as a compensatory response to OA (Hüning et al. 2013; Carreiro-Silva et al. 2014; Goncalves et al. 2017; Downey-Wall et al. 2020; Strader et al. 2020; Rajan et al. 2021; Schwaner et al. 2022a, b). When exposed to high  $p\text{CO}_2$ , sea urchins (*Paracentrotus lividus*) upregulate genes associated with calcification and metabolism (Martin et al. 2011), while larval Portuguese oysters (*C. angulata*) and larval Pacific oysters (*C. gigas*) overexpress genes involved in shell formation (Yang et al. 2017; De Wit et al. 2018) to sustain biomineralization under altered carbonate chemistry. In addition, genes related to ion and acid–base regulation in the pearl oyster (*Pinctada fucata*) are upregulated under OA, suggesting the implementation of a compensatory acid–base mechanism to mitigate adverse effects of low pH (Li et al. 2016). Changes in gene expression associated with acclimation to stressful environmental conditions can protect populations from immediate threats until resilient genotypes can be selected.

Acclimation to environmental perturbations can provide short-term protection; however, physiological plasticity often has associated trade-offs. When exposed to acidification, the coral polyp (*Acropora millepora*, Moya et al. 2012) and larval sea urchin (*Strongylocentrotus purpuratus*, O'Donnell et al. 2010) downregulate genes involved in metabolism, indicating metabolic suppression under OA stress. The Korean mussel (*Mytilus coruscus*) downregulates genes related to shell matrix for  $\text{CaCO}_3$  crystal formation and growth (Zhao et al. 2020), resulting in weakened shells. For this reason, while plasticity may offer an important means of resilience for populations facing immediate changes, evolutionary adaptations will still be essential for persistence into the future.

Natural genetic variation is a valuable source of resilience to changing environments (Hermisson and Pennings

2005; Barret and Schluter 2008; Bitter et al. 2019). Oysters are generally highly polymorphic and their genomes contain a wide range of genes enabling them to respond to environmental perturbations (Zhang et al. 2012a, 2016; Powell et al. 2018), which is a prerequisite for adaptation to changing environments. Evolutionary response to OA will most likely occur in areas with large populations and variable pH, such as estuarine habitats of oysters. An example of this can be found in sea urchins that are locally adapted to pH gradients caused by upwelling along the Pacific coast of North America (Kelly et al. 2013). In that study, differences in acidification regimes acted to maintain genetic variation required to enable adaptation to altered carbonate chemistry (Kelly et al. 2013). Capacity of organisms to adapt to fast-paced environmental changes is relatively unknown, but evidence suggests that there might be circumstances where natural or artificial selection could result in populations of individuals better suited to withstanding OA (Parker et al. 2011; Pespeni et al. 2013; Goncalves et al. 2017; Thomsen et al. 2017). For example, Thomsen et al. (2017) demonstrated differences in survival between different populations of mussels exposed to OA stress, revealing that local carbonate chemistry can influence the response of mussel populations to experimental acidification, suggesting local adaptation. In addition, Pespeni et al. (2013) showed that OA produces patterns of genome-wide selection in purple sea urchins (*Strongylocentrotus purpuratus*) reared in different  $\text{CO}_2$  conditions. Understanding if OA resilience is genetically determined, and if so, identifying molecular markers that could be used to breed more resilient organisms, while maintaining genetic variability (marker-assisted selection) can ensure healthy populations of oysters to benefit the economy, contribute to food security, provide natural shoreline protection, and improve water quality and overall ecosystem health.

This study was designed to provide novel insights into the capacity of the eastern oyster to respond to future climate change and identifies the mechanisms by which this response occurs. Adult oysters were spawned and resulting offspring were reared in control and acidified conditions for 3 months, and samples of larvae and juveniles were sampled for RNA and DNA sequencing, viability, and growth. Transcriptomic analysis (RNA sequencing or RNAseq) of larvae and juveniles was performed to identify genes that are differentially regulated in response to OA. Genomic analysis (restriction site associated DNA sequencing or RADseq) was also performed on juveniles to identify alleles associated with better survivorship under acidification. Results allowed the identification of potential molecular mechanisms associated with resilience to acidification in the eastern oyster. This is the first study in eastern oysters to combine RNA and RAD sequencing to identify novel candidate genes for resilience to OA.

## Materials and Methods

### Sample Collection

Ripe adult oysters were collected from Islip, NY (40°42'19" N, 73°11'32" W) and conditioned for spawning (Helm et al. 2004). Sperm and eggs were mixed from six females and six males. After allowing sufficient time for fertilization (1 h), embryos (16 million) were moved to aquaria (4 replicates/condition) equilibrated with CO<sub>2</sub> mixed with air (via a gas proportionator system; Schwaner et al. 2020; Schwaner et al. 2022a) or ambient air to attain the following two target *p*CO<sub>2</sub> levels: (1) low *p*CO<sub>2</sub>/high pH (control), pH 7.98, *p*CO<sub>2</sub> 480, and (2) high *p*CO<sub>2</sub>/low pH (acidified), pH 7.57, *p*CO<sub>2</sub> 1374. The CO<sub>2</sub> gas mixtures from the proportionator system were delivered to the bottom of each aquarium, resulting in similar seawater chemistry between replicates. Samples of seawater for dissolved inorganic carbon (DIC) analysis were obtained before introduction of larvae into the seawater, during larval development, and post-metamorphosis (Suppl. Tables 1–2). DIC samples were assessed using an EGM-4 Environmental Gas Analyzer® (PP systems) after acidification and separation of the gas phases using a Liqui-Cel® Membrane (Membrana) (provided by the Gobler laboratory at Stony Brook University). For quality assurance, before and after analysis, certified reference material (provided by Andrew Dickson, Scripps Institution of Oceanography) was analyzed with a 99.9% recovery. Total alkalinity,  $\Omega_{\text{aragonite}}$ ,  $\Omega_{\text{calcite}}$  carbonate concentration, and *p*CO<sub>2</sub> were determined in R using the package *seacarb* with known first and second dissociation constants of carbonic acid in seawater (Millero 2010). Larvae were reared following methods described in Schwaner et al. (2020; 2022a), with specific recommendations for *C. virginica* from Helm et al. (2004). Viability was monitored during every water change (3–5 times/week) by assessing ciliary movement microscopically, and growth samples were collected on days (1, 2, 5, and 8) and fixed with glutaraldehyde (1%) for analyses using ImageJ (Version 1.44, NIH). After 96 h in the *p*CO<sub>2</sub> conditions, larvae were concentrated on a 50-micron sieve, rinsed to remove detritus, checked for viability, and then, one million larvae (4 million/condition) were collected and stored at –80 °C for RNA sequencing (time 96 h) (Suppl. Figure 1). The remaining larvae were kept in either control or acidified conditions (4 million/condition, one million/replicate). When oysters reached 200 microns in size, a PVC sieve was inserted into the aquaria with shell chips or “cultch” layered on the sieve, so that oysters were able to settle out of the water column and attach to shell pieces. After settlement, juvenile viability was monitored and dead oysters were removed from tanks. At 1 and

2 months post fertilization, average size of oysters was assessed by taking a subsample for image analysis. After 3 months post fertilization, 60 individual juveniles (15/replicate) were randomly collected from each condition (total of 120) and stored at –80 °C (time 3 months) for RADseq. A second sample was taken for RNA sequencing.

### DNA and RNA Extractions

DNA was isolated from individual 3-month-old juvenile oysters (15 individuals/replicate, 4 replicates/condition, 120 total) using standard phenol–chloroform extraction (Farhat et al. 2020; Schwaner et al. 2022a; Boutet et al. 2022).

RNA was separately extracted from the 96-h and 3-month-old oysters (Suppl. Figure 1). For the time 96 h sample, pelleted larvae (1 pool/replicate, 4 pools/condition) were thawed in 800 µl of TRIzol Reagent (Invitrogen, Thermo Fisher Scientific, Waltham, MA) and homogenized with ceramic beads using a Fisherbrand™ Bead Mill 24 Homogenizer (Thermo Fisher Scientific). After homogenization, samples were incubated for 10 min in TRIzol and then 100 µl of 1-bromo-3-chloropropane was added. The solution was incubated for 10 min and centrifuged (20 min, 4 °C, 14,000 g). Isopropanol was added (1:1 ratio) to the aqueous phase, followed by a 10-min incubation and spin (10 min, 4 °C, 14,000 g). The supernatant was discarded, and the pellet was washed with 75% ethanol and then centrifuged (5 min, 4 °C, 14,000 g). The pellet was air dried for 5 min and dissolved in 50 µl of RNase-free water. RNA samples were cleaned using the sodium acetate precipitation protocol coupled with polyvinylpyrrolidone, 2% (w/v). Finally, DNA was removed using DNA-free™ Kit (Ambion, Thermo Fisher Scientific), following manufacturer's protocols. Purity of RNA was checked on a NanoDrop® ND-1000 Spectrophotometer (Thermo Fisher Scientific).

Juveniles sampled at 3 months were pooled (10 oysters/replicate, 4 pools/condition), thawed in lysis buffer, homogenized using the Bead Mill 24 Homogenizer, and RNA was extracted using the RNeasy Plus Mini Kit following manufacturer's instructions (Qiagen, Hilden, Germany). Cleaning and DNA removal were performed as outlined above.

### ddRAD Library Preparation

ddRAD libraries were prepared using a modified protocol from Peterson et al. (2012) and Schwaner et al. (2022a). Briefly, 200 ng of each DNA sample was double digested with PstI high fidelity restriction endonuclease and MseI or with AciI, MspI, HpyCH4IV, and KasI in a 25-µl reaction containing Cut Smart Reaction Buffer 10× (New England Biolabs, Ipswich, MA) and water at 37 °C for

10 h. After 10 h at 37 °C, the enzymes were inactivated by heating at 65 °C for 20 min. Each of the digested DNA samples was individually identified through the ligation of P1-n barcoded adapters at 16 °C for 6 h in a 30- $\mu$ l reaction containing P1 adapter, T4 DNA ligase, ATP, P2 adapter, and CutSmart reaction buffer. Samples were purified, and size was selected using Nucleomag NGS clean-up and size select kit (Macherey–Nagel, Düren, Germany) at 1:1 ratio of beads to sample and resuspended in Tris buffer. Purified adapter-ligated fragments were PCR-amplified with 12 uniquely indexed PCR-P2 primer sequences for multiplexing. Each individual sample had a distinct combination of index and barcode allowing for post-sequencing demultiplexing. Quality control of PCR products was checked using gel electrophoresis and Qubit dsDNA HS assay kit (Life Technologies, Thermo Fisher Scientific). After quantification, samples were pooled and precipitated. The two libraries were combined (40% PstI/MseI, 60% AciI, MspI, HpyCH4IV/KasI; 800 ng per line in 30  $\mu$ l of H<sub>2</sub>O), and then, size was selected with Pippin-Prep (1.5% agarose dye free gel cassette, Sage Science, Beverly MA, USA) under a setting with a range of 320–900 bp. Each fraction (320–600 bp, 320–800 bp, 350–800 bp, 400–800 bp, 500–900 bp) was quantified with Qubit, and quality was checked on a Bioanalyzer with high-sensitivity DNA chip (Agilent technologies, Waldbronn, Germany). To have better repartition, a larger range of sizes and better representativity of each size fraction, 20% of the 320–800 bp, 40% of the 400–800 bp, and 40% of the 500–900 base pair cut, were added to the library for sequencing. Five percent of PhiX control libraries were used to create a more diverse set of clusters as recommended by Illumina for the sample type. Samples were sequenced using Illumina NovaSeq 6000 System (Illumina, San Diego, CA) with an S4 flow cell on one lane, generating 2,872,893,796 paired-end (PE) 150 bp reads total.

### SNP Analysis

PE reads were demultiplexed by index at the sequencing facility (Novogene, UC Davis, Sacramento, CA). Reads were further demultiplexed by barcode into individual samples, using CLC Workbench (version 11.0.1, CLC Bio, Aarhus, Denmark, (<https://digitalinsights.qiagen.com/>) with default parameters. Sequence reads were trimmed based on quality scores (limit 0.05), ambiguous nucleotides (max 2 nucleotides per sequence), and adapters. Reads were mapped onto the *C. virginica* reference genome with default parameters (GCF\_002022765.2\_C\_virginica-3.0 downloaded from NCBI) using CLC. Unaligned ends were realigned with three multi passes using guiding variants. BAM files were exported from CLC, and variants were identified using Stacks v2 with the ref\_map pipeline (Rochette et al. 2019). Data filtering for

detection of high-quality SNPs included: minimum allele frequency 0.05 (–min-maf), a minimum percentage of samples in the population (75%) (–min-pop), and a HWE  $p$ -value < 0.05 (–hwe) (Farhat et al. 2020). The “populations” program within stacks calculates population genetic statistics for populations in the processed dataset (Suppl. Table 3). After filtering, only SNPs that had significantly higher  $F_{ST}$  between the compared populations values were selected (corrected AMOVA  $F_{ST}$  > 0.05 and  $p$  < 0.05). The significant SNPs were annotated using the *C. virginica* gff file from NCBI (GCF\_002022765.2). To identify positively selected loci, three published selections scans were used: PCAdapt (Luu et al. 2017), BayeScan (Foll and Gaggiotti 2008), and OutFLANK (Whitlock and Lotterhos 2015). The outlier SNP loci detection was performed using wrapper functions of the R package *SambaR* (Jong et al. 2021). The position of each variant in the genome (intergenic, untranslated region, coding sequence, or intron) and the type of consequence the variant has on the gene (missense, synonymous, stop-gained) were then inferred as described previously in Farhat et al. (2020). PROVEAN (Protein Variation Effect Analyzer- predicts if an amino acid substitution will have an impact on biological function of protein) scores were calculated for select SNPs of interest (Choi et al. 2012). To visualize population structure, a minimum spanning network was used, which clusters multilocus genotypes by genetic distances between them (Grunwald et al. 2017).

### RNAseq Library Preparation, Sequencing, and Analysis

Extracted RNA was sent to Novogene for sequencing. One microgram RNA per sample was used as input material. Sequencing libraries were generated using NEBNext® Ultra™ RNA Library Prep Kit for Illumina® (New England Biolabs, Ipswich, MA), following manufacturer’s instructions and with indices added for demultiplexing of samples. Libraries were sequenced on Illumina platform (Novaseq 6000), and 150 PE reads were generated. Novogene performed quality control tests, and cleaned reads were used in downstream analyses. Read mapping was performed by using HISAT2 to map filtered sequenced reads to the reference genome (Kim et al. 2019). The reference genome and gene model annotation files were obtained from NCBI (GCA\_002022765.4). HTSeq v0.6.1 was used to count the number of reads mapped to each gene, and FPKM (Fragments Per Kilobase of transcript per Million mapped reads) was calculated (Putri et al. 2022). Differential gene expression analysis was conducted using the *EdgeR* package from Bioconductor (3.6.3) (Robinson et al. 2010). The analysis was performed on read counts to which normalization and dispersion factors were applied before conducting

tagwise tests. *P*-values were adjusted using the false discovery rate (FDR) keeping only the genes having an  $FDR < 0.05$ . Genes were further selected to only include those with log fold change  $> |2|$ . In addition, Gene Ontology (GO) annotation was performed and a GO enrichment analysis of differentially expressed genes was performed using the *topGO* R package (Alexa and Rahnenfuhrer 2020) using Fisher's exact test. GO terms with corrected *p*-value  $< 0.05$  were considered significantly enriched. To visualize RNAseq data, samples were plotted using principal component analysis, heat maps, and volcano plots.

## Results

### Viability and Growth

There were no significant differences in viability between larvae grown at control or acidified conditions ( $p$ -value  $> 0.05$ ; G-test of Independence;  $n = 4$ ) until 2 weeks post fertilization ( $p < 0.001$ ; Fig. 1). At 2 weeks, larvae from the acidified condition had significantly greater mortality than those grown under control conditions (Fig. 1). Mortality

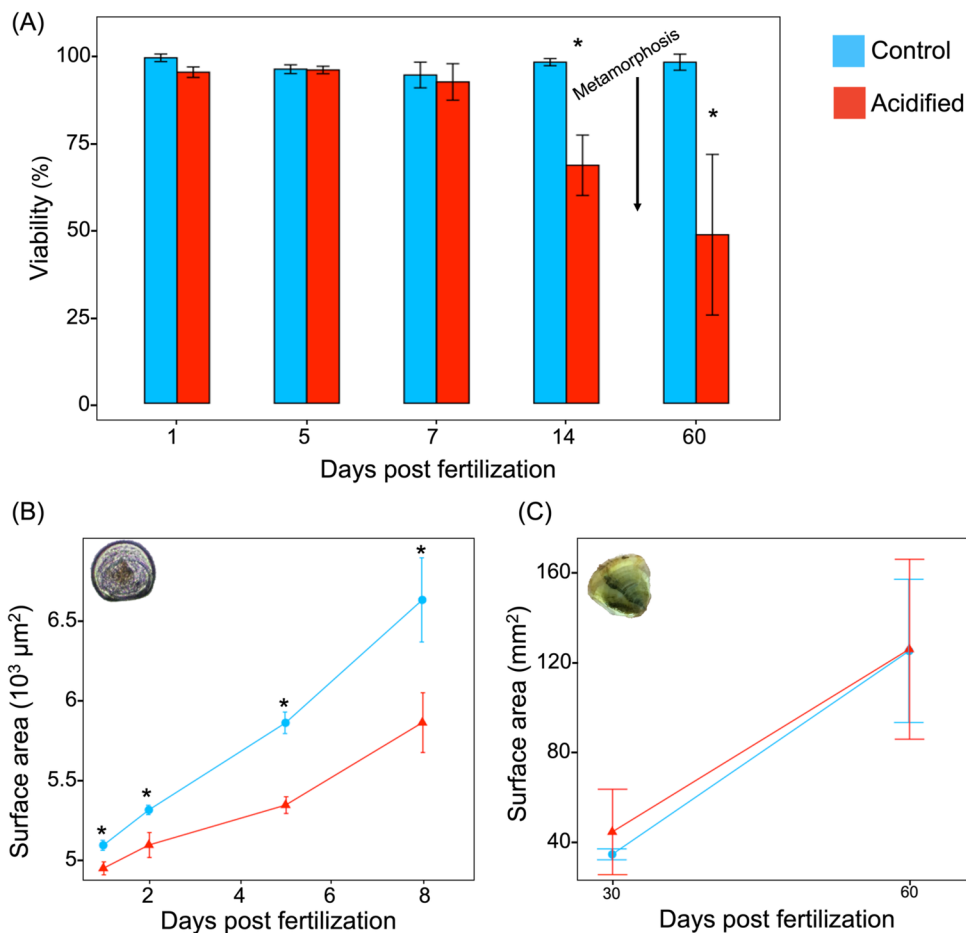
was negligible (2%) in metamorphosed juveniles grown under control conditions. In contrast, juveniles maintained under acidified condition continued to experience high mortality (52%; Fig. 1) underlining the selective pressure exerted by acidification ( $p < 0.001$ ).

Larvae grown under control conditions were systematically larger than those maintained under acidified conditions (Fig. 1), and differences were statistically significant 1 ( $p < 0.001$ ; nested-ANOVA), 2 ( $p = 1e - 04$ ), 5 ( $p < 0.001$ ), and 8 ( $p < 0.001$ ) days post fertilization. This trend did not continue post metamorphosis, as no difference in growth was noted for the 30- and 60-day sampling points (Fig. 1).

### Overall Variant Detection

Mapped reads averaged  $23,054,410 \pm 5,968,450$  per oyster for control juveniles and  $23,662,172 \pm 6,265,357$  for acidified juveniles. SNPs were identified in each subpopulation (Suppl. Table 4), and significant variants were further analyzed (Suppl. Table 5). Significant SNPs were detected between  $pCO_2$  conditions. The clustering of the samples (control and acidified) according to variant frequency

**Fig. 1** Survivorship (A), growth (shell surface area) in oyster larvae (B) and juveniles (C) in oysters exposed to control (blue) or acidified (red) conditions. The asterisks denote significant differences between control and acidified. Error bars are  $\pm$  standard error of the mean



showed a grouping based on the  $p\text{CO}_2$  condition for juvenile samples (Fig. 2).

In order to target pathway processes under selection by acidification, the positions of the significant SNPs in the different regions of the genome (coding sequences, untranslated region, intron, intergenic region, Suppl. Table 6) were identified. Furthermore, the variant consequences for the predicted proteins (i.e., if the variant induces a stop codon, missense variant, or synonymous variant, Suppl. Tables 7–8) were deduced. A total of 2258 variants were identified in the coding regions (CDS) in juvenile oysters (control vs acidified condition), including 756 synonymous, 236 missense, and 1151 stop-gained variants (Suppl. Tables 7, 8). BayeScan detected 2 outlier SNPs, PCAdapt detected 8, OutFLANK detected 68, with none present in all three comparisons (Suppl. Table 9; Suppl. Figure 2).

Overall, the significant SNPs were found in genes coding for proteins mediating several biological processes, many of which are known to be influenced by OA. Broadly, these groups will be referred to as (1) biomineralization and  $\text{Ca}^{2+}$  transport; (2) hemocyte function; (3) cytoskeleton, extracellular matrix, cell matrix adhesion; (4) immune and stress response; and (5) growth and development (Table 1).

## DEGs Identified in Control vs Acidified Larvae

Significant differences were noted in the transcriptional profiles of larval oysters reared under acidified conditions as compared to control larvae (Suppl. Figures 3–5). Mapped RNAseq reads averaged  $30,903,826 \pm 4,700,828$  reads per pool for controls and  $33,589,2982 \pm 2,436,150$  for acidified larval groups. In response to acidification, 753 genes were found to be differentially expressed: 319 were upregulated, while 434 were downregulated in the acidified condition (Suppl. Table 10). However, 480 (63.75%) of the identified genes had uncharacterized function. Annotated upregulated genes were categorized using gene ontology (GO) and are represented in Fig. 3A. GO analysis showed overrepresentation in several functional groups including microtubule cytoskeleton, cell death and apoptosis, metabolism, and gene expression.

Genes upregulated in larvae encompassed some that had the same gene description as genes containing SNPs enriched in juveniles (Table 1; Suppl. Table 10), including genes coding for proteins related to biomineralization (receptor-type tyrosine-protein phosphatase epsilon-like, mucin-5AC-like, short-chain collagen C4-like), hemocyte function (protein draper-like), cell adhesion (microfibril-associated

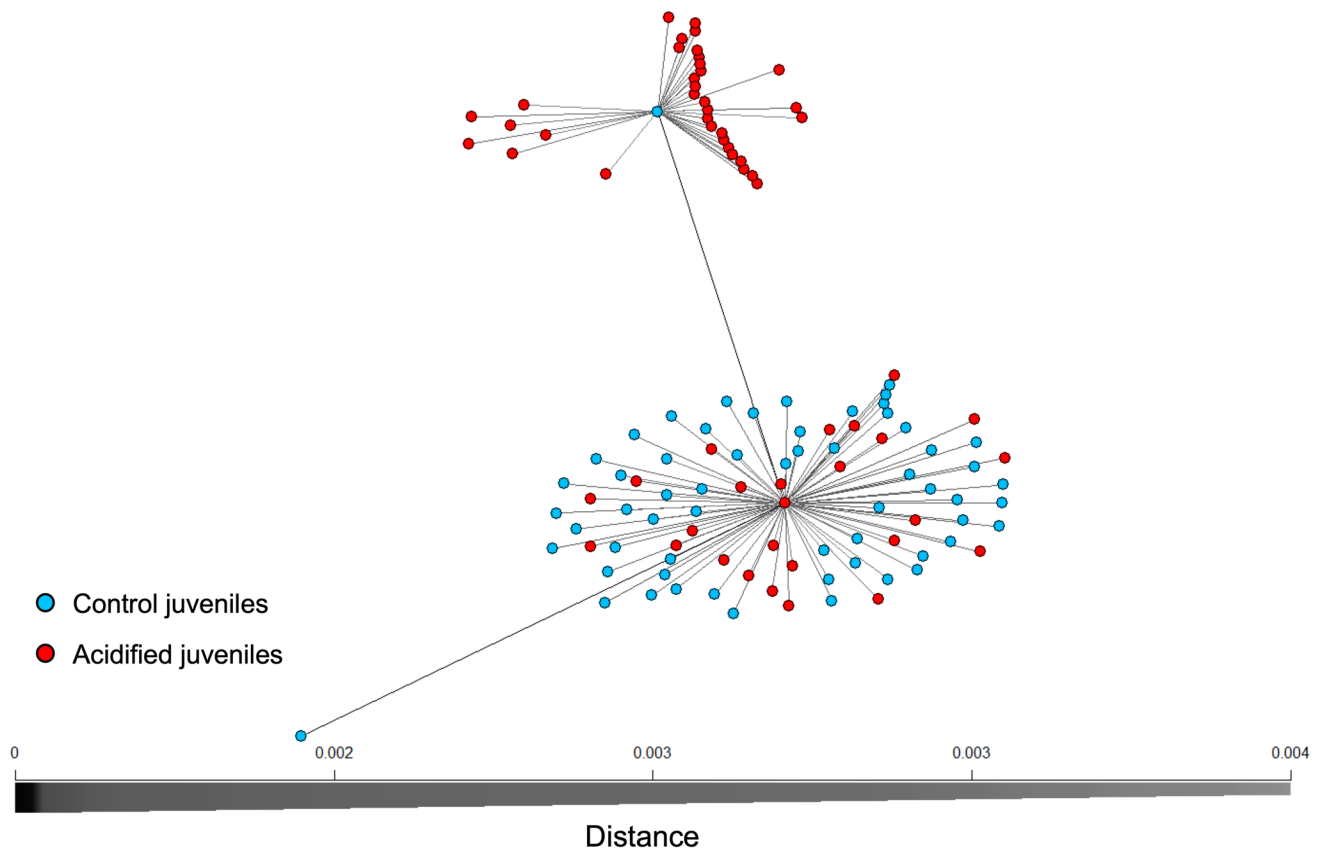


**Fig. 2** Clustering based on the frequency of filtered SNPs at the juvenile stage ( $n = 60$  oysters/treatment) from control and acidified conditions

**Table 1** Variants in juvenile oysters from acidified conditions and DEGs with probable functions related to biomineralization, Ca<sup>2+</sup> transport, hemocyte function, cytoskeleton/extracellular matrix/cell adhesion, immune and stress response, and growth and development.

\*Significant after at least one outlier test. Up arrow: enriched in acidified, down arrow: depleted in acidified. For DEGs, empty cells designate genes that were not significantly regulated, and log fold change (LFC) is noted for differentially expressed genes

Protein function	Gene ID	SNPs	DEGs	
			Juvenile	Larvae
<b>Biom mineralization</b>			<b>LFC</b>	<b>LFC</b>
Fibroblast growth factor receptor 2-like	111129975	Stop gained ↑		
Pleckstrin homology-like domain family B member 2	111122811	Stop gained ↑		
BTB/POZ domain-containing protein 19-like	111128284	Stop gained ↑		
Extensin-like	111106495	Stop gained ↑		
Short-chain collagen C4-like	111121618	Missense ↓		
	1111075961	Stop gained ↓		
	111112590		-3.69	
Protein PIF-like	111116492	Synonymous ↓		
Mucin-19-like	111117026	Stop gained ↓		
Receptor-type tyrosine-protein phosphatase alpha-like	111117327	Stop gained ↓		
Receptor-type tyrosine-protein phosphatase epsilon-like	111112166	Missense ↑		
	111112059	Synonymous ↑		
	111130194	Stop gained ↓		
	111116874			2.93
Mucin-5AC-like	111112476	Stop gained ↑		
	111137674			2.46
Perlucin-like protein	111111960		6.30	
	111102603		6.58	
	111110737			4.8
	111128827			3.12
Laminin subunit alpha-like	111111933			4.72
C-type lectin domain family 4 member E-like	111115169			2.45
Tyrosinase-like protein	1111114108			5.07
Carbonic anhydrase	111117514			2.3
<b>Ca ion transport</b>				
VWFA and cache domain-containing protein 1-like	111129463	Stop gained ↑		
Agrin-like	111132939	Synonymous ↑		
Serine/threonine-protein phosphatase 6 regulatory ankyrin repeat subunit B-like	111114383	Synonymous ↑		
Probable phosphorylase b kinase regulatory subunit alpha	111123775	Synonymous ↑↓		
V-type proton ATPase 21 kDa proteolipid subunit-like	111118152	Synonymous ↓		
NMDA receptor synaptonuclear signaling and neuronal migration factor-like	111127669	Stop gained ↓		
Inositol 1 2C4 2C5-trisphosphate receptor type 2-like	111135721	Synonymous ↓		
Neurogenic locus notch homolog protein 1-like	111107254	Missense ↓		
E3 ubiquitin-protein ligase UBR4-like	111122987	Stop gained ↑↓		
NADPH oxidoreductase A-like	111099152	Synonymous ↑		
Trichohyalin-like	111133205	Synonymous ↑,		
	111125797	Stop Gained ↑		
	111113331	Missense ↓		
	111115648			-4.44
Neurogenic locus notch homolog protein 1-like	111107506	Stop gained ↑		
	111107254	Missense ↓		
Aggrecan core protein-like	111117161			4.36
<b>Hemocyte function</b>				
Protein draper-like	111117670	Missense ↑		
	111104411			2.61
	111113084			3.26

Table 1 (continued)

Protein function	Gene ID	SNPs	DEGs	
			Juvenile	Larvae
	111110468			3.97
	111112543			4.92
Ankyrin-1-like	111112668	Missense ↑		
<b>Cytoskeleton</b>				
tctex1 domain-containing protein 1-like	111108835	Synonymous ↑		
Kinesin-like protein KIFC3	111136219	Stop gained ↑		
Disks large homolog 1-like	111099483	Synonymous ↑		
Filamin-A-like	111107913	Stop gained ↑		
Tropomodulin-like	111114836	Synonymous ↑		
Rho-related protein racA-like	111114627	Synonymous ↓		
Unconventional myosin-VIIa-like	111121714	Synonymous ↓		
Unconventional myosin-Va-like	111111058	Stop gained ↓		
Dynein heavy chain 7 2C axonemal-like	111124938	Synonymous ↓		
Dynein heavy chain 6 2C axonemal-like	111113098	Stop gained ↓		
Chromosome-associated kinesin KIF4-like	111127380	Synonymous ↓		
Dynein beta chain 2C flagellar outer arm-like	111122795	Stop gained ↓		
Myosin-10-like	111126599	Stop gained ↓		
Spectrin beta chain-like	111130534	Stop gained ↓		
Adenomatous polyposis coli protein-like	111111223	Stop gained ↓		
Protein SON-like	111100490			4.51
Keratin, type I cytoskeletal 9-like	111137526			6.72
Loricrin-like	111110617			5.84
<b>Extracellular matrix proteins</b>				
Extracellular matrix protein FRAS1-like	111119697	Synonymous ↑		
Prolyl 4-hydroxylase subunit alpha-1-like	111125537	Missense ↓ Synonymous ↓		
Coadhesin-like	111105725	Synonymous ↓		
Tensin-1-like	111113215	Stop gained ↓		
Fibrillin-1-like	111108443	Stop gained ↑		
Hemicentin-1-like	111124194	Stop gained ↓		
	111122975			3.88
Fibropellin-3-like	111116829			2.8
Latent-transforming growth factor beta-binding protein 1-like	111127029			3.81
Transforming growth factor-beta-induced protein ig-h3-like	111115388			3.34
<b>Cell matrix adhesion</b>				
Down syndrome cell adhesion molecule homolog	111125387	Synonymous ↑		
Cadherin EGF LAG seven-pass G-type receptor 3-like	111108340	Synonymous ↑		
	111118941			2.94
Protocadherin gamma-B4-like*	111125407	Stop gained ↓		
Protocadherin beta-3-like*	111125408	Missense ↓		
Nectin-1-like	111101367	Missense ↓		
Interaptin-like	111134844	Synonymous ↓		
Fasciclin-1-like	111112294	Synonymous ↓		
Microfibril-associated glycoprotein 4-like*	111129564	Synonymous ↑		
	111136853	Stop gained ↑		
	111134246			4.97
Protein mesh-like	111132905	Missense ↑		
Serine-rich adhesin for platelets-like	111124862	Synonymous ↓		
	111108355	Stop gained ↓		
	111137278			2.69



**Table 1** (continued)

Protein function	Gene ID	SNPs	DEGs	
			Juvenile	Larvae
<b>Immunity</b>				
Lactose-binding lectin 1-2-like	111137862	Stop gained ↑		
Antistasin-like	111115654	Stop gained ↑		
Baculoviral IAP repeat-containing protein 2-like	111123894	Stop gained ↑		
	111100408			-2.09
Toll-like receptor 2	111119086	Synonymous ↓		
	111116845			-3.53
	111112142			-4.58
Toll-like receptor 13	111105058			-4.04
Toll-like receptor 6	111124179	Synonymous ↓		
	111117598			-3.76
Fibrinogen C domain-containing protein 1-like*	111126623	Stop gained ↓		
	111124855			-5.36
	111111092			-2.74
Immune-associated nucleotide-binding protein 9-like	111108219	Stop gained ↓		
Cell death abnormality protein 1-like	111116135	Stop gained ↓		
	111119721			-2.4
	111100322			-3.65
Histone H1.0-like	111124711	Synonymous ↑		
IgGFc-binding protein-like	111125889	Stop gained ↑		
	111124183			6.01
	111109297			-5.21
E3 ubiquitin-protein ligase TRIM56-like	111124756	Synonymous ↓		
E3 ubiquitin-protein ligase TRIM71-like*	111107259	Missense ↑		
Baculoviral IAP repeat-containing protein 3-like	111100471			-2.47
Baculoviral IAP repeat-containing protein 8-like	111104229			-2.37
Immune-associated nucleotide-binding protein 12-like	111103088			-5.16
CD209 antigen-like protein A	111114480			-5.31
Techylectin-5A-like	111113971			-4.99
Ficolin-1-like	111112465			-4.53
Ficolin-2-like	111108103			-2.92
Fucoatlectin-like	111109173			-3.84
Scavenger receptor cysteine-rich type 1 protein M130-like	111117277			-3.01
Scavenger receptor class A member 5-like	111116991			-8.08
Galectin-3-binding protein A-like	111134744			-2.69
Interferon-induced protein 44-like	111110991			-4.86
	111116003			-2.21
FK506-binding protein 2-like	111127442			-3.22
Glycine receptor subunit alpha-2-like	111122821			-3.17
Neuropeptide-like protein 29	111130994			-3.16
	111130993			-2.22
Waprin-Phi1-like	111126768			-2.98
2'-5'-oligoadenylate synthase 1A-like	111104300			-2.36
<b>Stress response</b>				
Tetratricopeptide repeat protein 25-like	111128582	Stop gained ↑		
G2 and S phase-expressed protein 1-like	111107342	Missense ↑		
Peroxidasin-like	111119019	Stop gained ↓		
Tetratricopeptide repeat protein 37-like	111131294	Stop gained ↓		
Tetratricopeptide repeat protein 28-like	111099218	Synonymous ↑		

**Table 1** (continued)

Protein function	Gene ID	SNPs	DEGs	
			Juvenile	Larvae
Heat shock 70 kDa protein 12A-like	111125389	Stop gained ↑		
	111125313	Stop gained ↓		
	111116119		-2.94	
	111114216			3.63
	111106970			-6.63
	111100169			-5.33
Polycystin-2-like	111104855		-4.93	
	111138465	Synonymous ↑		
Heat shock protein 70 B2-like	111119513			-3.22
	111119512			-2.93
	111108251			-2.57
	111120887			-2.5
Heat shock protein 27-like	111137387			-2.04
Cell wall integrity stress response component 1-like	111117439			5.27
WSC domain-containing protein ARB_07870	111118674			5.32
Peroxidase-like protein 3	111101491		-3.51	
Peroxidase-like protein	111099782			-2
	111123816			2
<b>Growth and development</b>				
Multiple epidermal growth factor-like domains protein 6	111116091	Stop gained ↑		
Frizzled-4-like	111103593	Synonymous ↑		
Rotatin-like	111135621	Stop gained ↑		
Putative ATP-dependent RNA helicase	111103568	Stop gained ↑		
Telomerase reverse transcriptase-like	111125755	Stop gained ↑		
Intraflagellar transport protein 46 homolog	111126300	Synonymous ↓		
Nephrocystin-3-like	111124940	Stop gained ↓		
Histone H4 transcription factor-like	111126953	Synonymous ↑		
		Missense ↓		
MYCBP-associated protein-like	111102249	Missense ↑		
Cilia- and flagella-associated protein 54-like	111107716	Missense ↑		
	111107620	Synonymous ↓		
	111099818	Missense ↑		
Cholecystokinin receptor type A-like		Synonymous ↑		
Multiple epidermal growth factor-like domains protein10	111113250		4.82	
	111112871		4.82	
	111114401			6.98
	111112167			9.89
Blastula protease 10-like	111115048			2.91
Semaphorin-5A-like	111104250			2.18
Chorion-specific transcription factor GCMb	111121596			3.88
THAP domain-containing protein 1-like	111109088			4.74
Multiple epidermal growth factor-like domains protein 11	111133416			2.87
	111102929			3.55

glycoprotein 4-like, serine-rich adhesin for platelets-like), and stress (heat shock 70 kDa protein 12A-like). In addition, genes upregulated in larvae included some that did not code for the same proteins as those that contained SNPs (Table 1) but had similar functions. This is the case for C-type lectin domain family 4 member E-like, tyrosinase-like protein 1,

carbonic anhydrase, and aggrecan core protein-like, all of which being involved in biomineralization and calcification.

Downregulated genes in larvae exposed to high  $p\text{CO}_2$  included some of the same functional groups as genes containing SNPs depleted under OA conditions in juveniles (Table 1; Suppl. Table 10), including trichohyalin-like

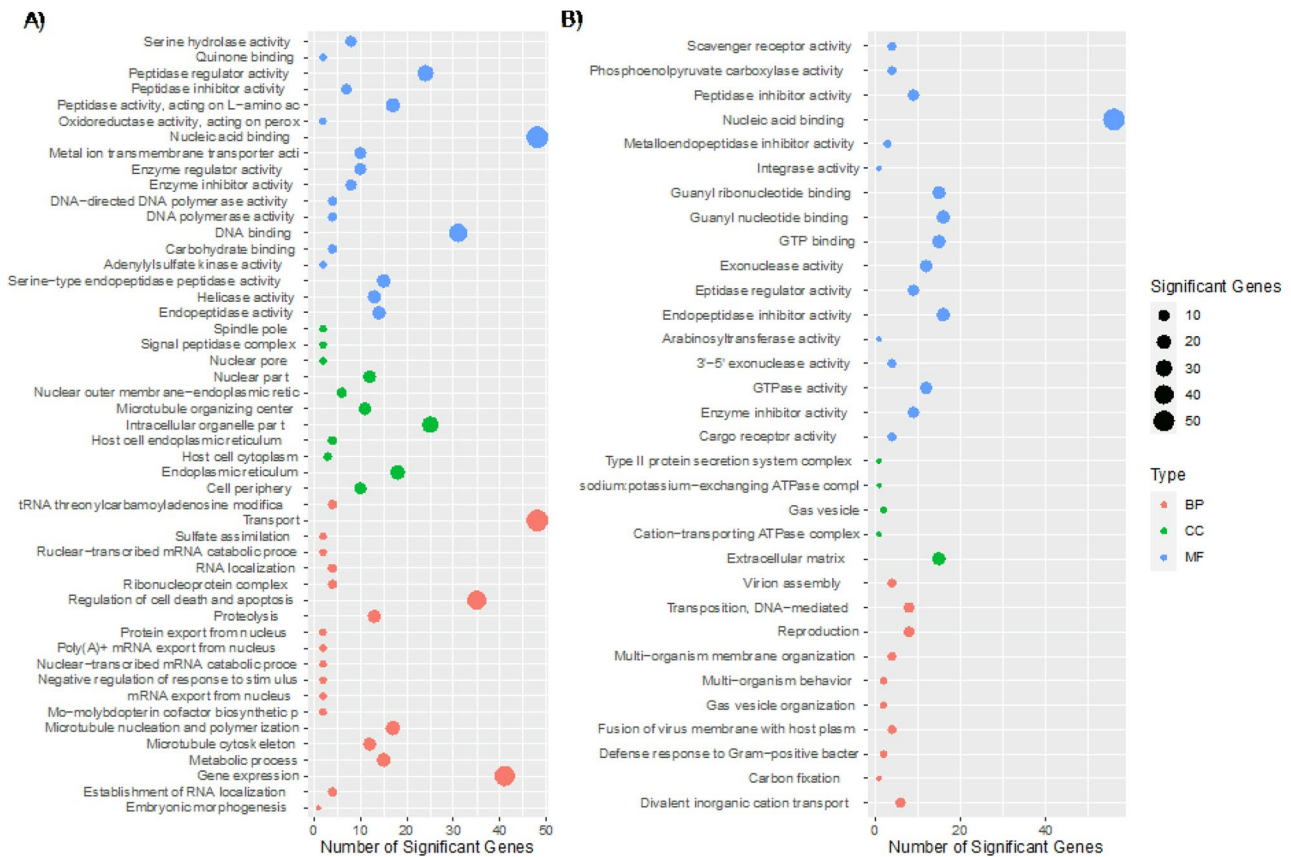


**Fig. 3** Number of upregulated (A) and downregulated (B) genes related to overrepresented GO terms in acidified larvae. BP, biological processes; CC, cellular components; MF, molecular function. Circle diameter represents number of genes

(Ca<sup>2+</sup> transport), toll-like receptor 2, fibrinogen C domain-containing protein 1-like, cell death abnormality protein 1-like, and heat shock 70 kDa protein 12A-like (immune and stress response). Of the downregulated genes (with known function) in larvae exposed to high pCO<sub>2</sub>, 19% were related to immune response (Table 1). These included genes such as big defensin-like and heat shock protein 70 B2-like. Figure 3B shows GO terms associated with downregulated genes, including immune processes such as defense response to bacteria, scavenger receptor activity, and enzyme inhibitor activity.

### Variants and DEGs Identified in Control vs Acidified Juveniles

Genes enriched with variants in acidified juveniles represented a total of 145 genes, with 98 (67.59%) and 47 (32.41%) of the genes having known and uncharacterized functions, respectively. These SNPs were found in proteins related to biomineralization, Ca<sup>2+</sup> binding and transport, hemocyte function, cytoskeleton/extracellular matrix/cell

adhesion, immune and stress response, and development (Table 1; Suppl. Table 8).

In addition to DNA sequencing, RNA sequencing was performed on the juvenile oysters in both conditions. Mapped RNAseq reads averaged 50,229,829 ± 23,476,626 reads for control and 51,981,350 ± 16,842,341 for acidified juvenile groups, and transcriptional profiles of these comparisons are shown in Suppl. Figures 6–8. In response to acidification, 340 genes were differentially expressed, with 134 and 206 transcripts upregulated or downregulated, respectively (Suppl. Table 11). Of these, 220 did not have a characterized function. Enrichment analysis showed several GO terms to be overrepresented among upregulated genes, including those related to immunity, Ca<sup>2+</sup> homeostasis, Ca<sup>2+</sup> channels, Ca<sup>2+</sup> transport, ion homeostasis, and cytoskeleton (Fig. 4A). Some of the upregulated genes also contained enriched SNPs. This was the case for the immune protein IgGfC-binding protein-like and the cell adhesion protein cadherin EGF LAG seven-pass G-type receptor 3-like.

Genes having variants depleted in juveniles exposed to acidified conditions (higher SNP frequencies in controls)

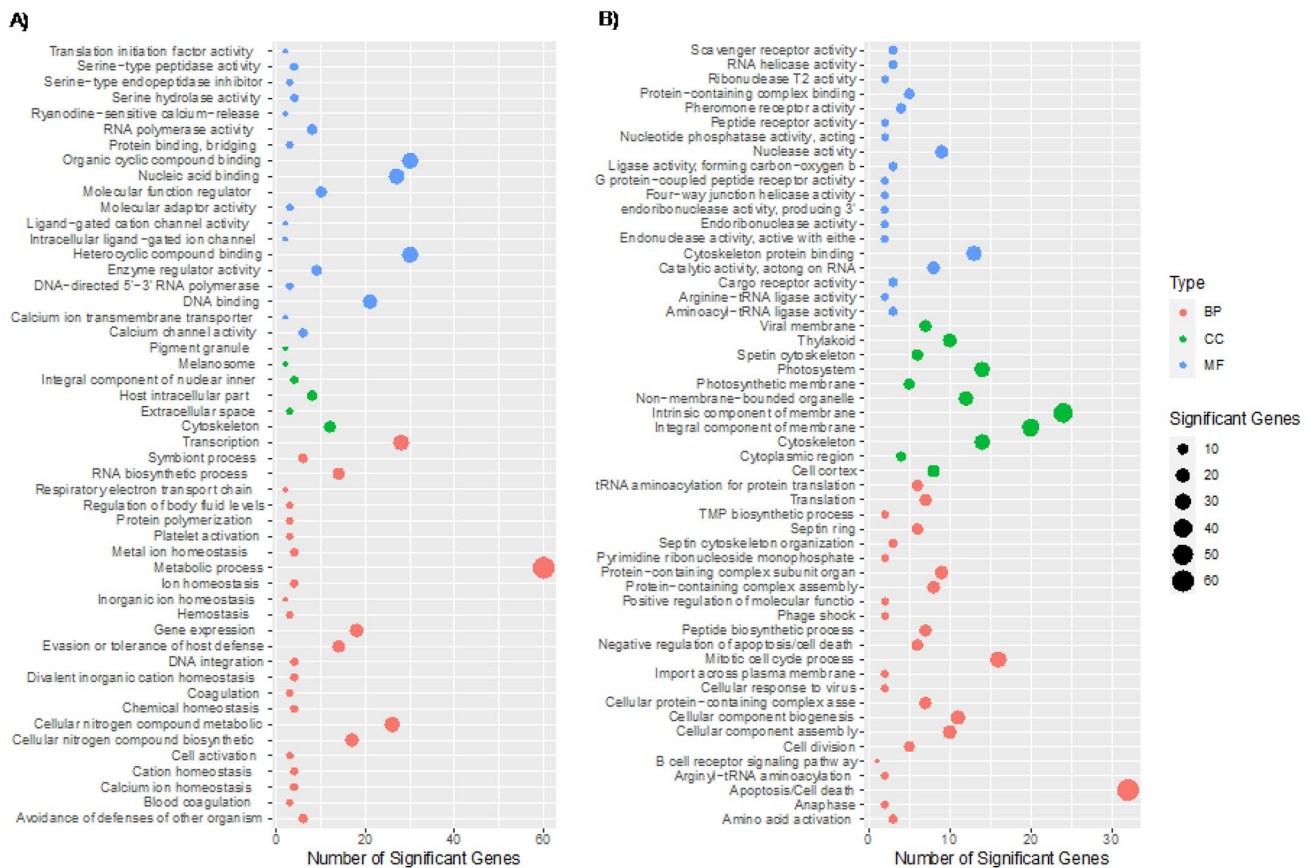


**Fig. 4** Number of upregulated (**A**) and downregulated (**B**) genes related to overrepresented GO terms in acidified juveniles. BP, biological processes; CC, cellular components; MF, molecular function. Circle diameter represents number of genes

represented a total of 178 genes, with 127 (71.35%) having known functions and 51 (28.65%) uncharacterized. The functional groups were generally similar between those depleted and enriched under OA (Table 1). These SNPs were found in proteins related to biomineralization (extensin-like protein, protein PIF-like, short-chain collagen C4-like), immune and stress response (fibrinogen C domain-containing protein 1-like and tetratricopeptide repeat protein 37-like proteins, toll-like receptor 6, fibrinogen C domain-containing protein 1-like, cell death abnormality protein 1-like, and heat shock 70 kDa protein 12A-like), and cytoskeleton (intraflagellar transport protein 46 homolog, dynein beta chain 2C flagellar outer arm-like, coadhesin-like, protocadherin gamma-B4-like proteins, myosin 10-like, dynein heavy chain 6, coadhesin-like, prolyl 4-hydroxylase subunit alpha-1-like, and protocadherin gamma-B4-like). Genes that were downregulated and also showed changes in SNPs frequencies included the proteins short-chain collagen C4-like, toll-like receptor 6, fibrinogen C domain-containing protein 1-like, cell death abnormality protein 1-like, and heat shock 70 kDa protein 12A-like. Most of the downregulated genes in acidified juveniles

were related to immunity and stress response, and 19% of all downregulated characterized genes were related to immune response (Table 1), such as peroxidase-like, fucolectin-like, ficolin-1-like, and ficolin-2-like. Downregulated GO terms included apoptosis, cell death, apoptotic signaling pathway, response to virus, and scavenger receptor activity (Fig. 4B).

## Discussion

### Distinct Genotypes of Juvenile Survivors of OA

After clustering the samples according to variant frequencies, results showed a distinct segregation of juvenile samples based on  $p\text{CO}_2$  condition, indicating genetic differentiation between the two groups as a result of acidification related mortalities. SNPs were found to have strong signatures of selection after  $F_{\text{ST}}$  outlier analysis by at least one analysis. The percent of SNPs identified as under selection was similar to that of the red abalone *Haliotis rufescens* (DeWit and Palumbi 2013), Pacific lamprey *Entosphenus tridentatus* (Hess et al. 2013), and the coral *Acropora*

*hyacinthus* (Bay and Palumbi 2014). Our study had a greater percentage of outlier SNPs than a similar study in sea urchin (*Strongylocentrotus purpuratus*) cultured under different  $p\text{CO}_2$  levels (Pespeni et al. 2013), in which the authors suggested high adaptation potential. Uthicke et al. (2019) investigated adaptation to OA in the tropical sea urchin (*Echinometra* sp.) and concluded that there was little evidence of adaptation to future OA based on the fact that most SNPs were silent substitutions without adaptive potential. SNPs in this study were mostly non-synonymous (missense and stop-gained). Usually, most amino acid substitutions are deleterious to the organism and are selected against, resulting in mostly synonymous substitutions (Palumbi and Oliver 2006). But selection can also maintain two functionally distinct types of protein in individuals in different environmental conditions, as we may have seen in our study, and in this case, there would be a large amount of non-synonymous substitutions (Palumbi and Oliver 2006). This was also seen in the non-synonymous variants of the RH1 gene in the sand goby (*Pomatoschistus minutus*) between Baltic and North Sea populations, which pointed to diversifying selection based on local marine environment instead of neutral processes (Larmuseau et al. 2010).

Taken together, our results suggest adaptation potential in the eastern oyster. Survival under chronic OA exposure appears to be, at least in part, due to selection of juveniles with specific genotypes that improve fitness.

### Mechanisms of Resilience by Life History Stage

There was no evidence of selection within the first 96 h of exposure to OA (still vulnerable phenotypes present), as supported by similar mortality and impacts of OA manifesting as reduction of growth that were reversed after selection in juveniles. Seven days of high  $p\text{CO}_2$  exposure were not long enough to induce selective mortality under our experimental conditions. Negligible mortality of larvae between  $p\text{CO}_2$  conditions within the first few days of exposure is similar to previous findings in the Pacific and eastern oysters (Timmins-Schiffman et al. 2013; Gobler and Talmage 2014). Even though they did not show differences in mortality before day 14, larvae reared in acidified conditions were significantly smaller than control larvae. Exposure to OA can cause a significant effect on larval development, such as reduced shell thickness and growth, that is not accompanied by immediate mortality (Gazeau et al. 2010), but could increase vulnerability at later stages and reduce settlement and metamorphosis success.

In nature, the spawning period for oysters in New York begins when seawater temperatures increase during summer months (Loosanoff 1966), coinciding with seasonal fluctuations in pH and extremes of acidification (Wallace et al. 2014; Baumann et al. 2015). Coastal areas can have

dramatic diel changes in pH, with pH amplitudes between 0.22 to 1.0 (Wallace et al. 2014; Baumann et al. 2015), so larvae may be more resilient to variable  $p\text{CO}_2$  than chronic exposure. Furthermore, *C. virginica* larvae were found to be capable of rebounding from high  $p\text{CO}_2$  stress when moved back to ambient conditions (Barbosa et al. 2022). Incorporating more levels of pH values, including a wider range, could have covered present and future environmental variability and would be interesting to investigate for future experiments. The larval oysters in this study had no difference in mortality until 2 weeks after fertilization, and there was a strong selective mortality post metamorphosis. RADseq data were generated after OA-related mortality and revealed significantly different SNP profiles between acidified and control oysters, while there were actually no more differences in growth at this stage, strongly supporting that the survivors actually represent more resilient individuals. Organisms have the ability to acclimate to OA within their lifetimes through various physiological mechanisms, including regulating gene expression (Todgham and Hofmann 2009; Hüning et al. 2013; Goncalves et al. 2017; De Wit et al. 2018). In this study, PCA of larval RNAseq data showed separation between  $p\text{CO}_2$  treatments that was less evident in juveniles, and larvae had over twice as many DEGs than juveniles. At the larval stage of development, acclimation appears to play a greater role in resilience, as there does not appear to be a selection of resilient genotypes until the juvenile stage. The juveniles in the acidified conditions were the same size as controls, whereas, during larval stages, they were much smaller. There appeared to be a selection for this larger phenotype. The acclimation of larva to OA may not be sustainable at the long-term, and could have associated physiological costs, which might explain the downregulated genes related to immunity. Our previous work demonstrated significant reduction in immunity in larva exposed to acidified conditions (Schwaner et al. 2020), suggesting that the high degree of plasticity in larvae may come at a cost.

Bivalve susceptibility to OA includes transient vulnerabilities specific to short-lived ontogenetic stages, such as formation of the initial shell within early larval development. Furthermore, the larval stage of oysters is pelagic while the juvenile stage is benthic, so the different life stages are exposed to different acidification stressors (Waldbusser and Salisbury 2014). Therefore, it is not surprising that sensitivity to OA in oyster larva may vary across developmental stages, and it is possible, rather likely, that mechanisms of resilience to OA may also depend on developmental stage. For instance, *C. gigas* larvae precipitate almost 90% of their body weight as  $\text{CaCO}_3$  in the first 48 h of development to form the D-hinge shell (Waldbusser et al. 2013). During this time, the calcifying surfaces have the greatest exposure to seawater (Waldbusser et al. 2013). At this stage, larvae rely on energy reserves so

it was hypothesized that initial shell development would be energetically constrained under OA (Waldbusser et al. 2013). Contrary to this suggestion, it has been demonstrated that regardless of the aragonite saturation state, *C. gigas* larvae utilize the same amount of total energy to complete first shell formation (Frieder et al. 2017), underlining the role of other process, such as specific genotypes or differential gene expression. However, later in development, studies have shown alterations in respiration and metabolism, which could indicate constraints from energetic demands under OA (Beniash et al. 2010; Pan et al. 2015). Altogether, these studies support our findings that mechanisms of resilience to OA likely vary by life history stage.

### Molecular Features Associated with Resilience to Acidification

Similar to this study, Bitter et al. (2019) and Pespeni et al. (2013) found multigenic adaptation to OA from variants across many different cellular pathways rather than just a few key genes. Molecular features resulting from this study were predominantly linked to biomineralization,  $\text{Ca}^{2+}$  transport, hemocyte function, cytoskeleton and its components, immune response, and development suggesting major adaptive mechanisms reside in these processes.

### Biomineralization and $\text{Ca}^{2+}$ Transport

The negative effects of OA on biomineralization among marine calcifiers have been well established (Gazeau et al. 2007; Thomsen et al. 2015; Zhao et al. 2017). Biomineralization is the process for producing  $\text{CaCO}_3$ , which makes up 95% of bivalve shells and is enabled by mantle tissue and hemocytes (Lowenstam and Weiner 1989; Mount et al. 2004). The concentration and availability of environmental  $\text{Ca}^{2+}$  and carbonate ( $\text{CO}_3^{2-}$ ) ions are essential to proper shell formation, and OA causes a disruption in the balance of carbonate species, leading to insufficient levels of  $\text{CaCO}_3$ . To compensate for this, organisms are able to alter the bioavailability of  $\text{CaCO}_3$  to promote calcification under low pH (Evans et al. 2013). Studies have previously demonstrated that bivalves can increase expression of genes involved in shell formation and  $\text{Ca}^{2+}$  transport to sustain biomineralization when experiencing acidification (Dineshram et al. 2015; Goncalves et al. 2017; Johnson et al. 2017; Yang et al. 2017; De Wit et al. 2018; Griffiths et al. 2019; Zhao et al. 2020), and SNPs have been detected at higher frequencies in biomineralization-related genes of the sea urchin (*Strongylocentrotus purpuratus*, Pespeni et al. 2013) and Mediterranean mussel (*M. galloprovincialis*, Bitter et al. 2019) under OA. For example, Goncalves et al. (2017) demonstrated 36-fold higher expression of perlucin, a protein found in the nacre organic matrix responsible for nucleation of  $\text{CaCO}_3$

crystals (Blank et al. 2003; Wang et al. 2008), in the Sydney rock oyster (*Saccostrea glomerata*) under OA stress. Perlucin was also upregulated under OA stress in the Manilla clam (Metzger 2012), Mediterranean mussel (Bitter et al. 2021), Mexican geoduck (Lopez-Landavery et al. 2021), and sea snails (Maas et al. 2015; Moya et al. 2016). Furthermore, RNA interference (RNAi) was used to validate the role of perlucin in resilience to OA in *C. virginica* (Schwaner et al. 2023). Here, perlucin-like was upregulated in both larvae and juveniles held under OA. Some C-type lectins, which include perlucin, have been identified as nacre proteins in mollusks (Marie et al. 2017), and C-type lectin domain has been identified as a common domain of molluscan shell proteins (Rajan and Vengatesen 2020). Pteropods exposed to OA for 10 h upregulated C-type lectin (Maas et al. 2015), and there was upregulation of C-type lectin domain family 4 member E-like in oyster larvae from acidified conditions. In a parallel study conducted in our lab, C-type lectin was upregulated in juvenile *Mercenaria mercenaria* under OA stress (Schwaner et al. 2022a).

A missense SNP was found in receptor-type tyrosine–protein phosphatase epsilon-like, at a higher frequency in juveniles from the acidified conditions compared to controls. Missense SNPs are non-synonymous and cause a change in the amino acid sequence which can affect protein function (Zhang et al. 2012b). Interestingly, this gene, in addition to the tyrosinase-like protein 1, was upregulated in larvae in response to OA. A synonymous SNP was also found in receptor-type tyrosine–protein phosphatase epsilon-like, with a higher frequency in acidified juveniles than controls. The impact of synonymous SNPs is often ignored, although it has been found that they can alter mRNA splicing, stability, structure, and protein folding which can affect protein function (Hunt et al. 2009). A missense SNP in receptor-type tyrosine–protein phosphatase beta was detected at a higher frequency in juvenile *M. mercenaria* survivors of 10 months of OA exposure compared to *M. mercenaria* maintained in ambient  $p\text{CO}_2$  (Schwaner et al. 2022a). Tyrosine is a periostracal protein (Hunt 1987), and tyrosine – protein phosphatase is an enzyme involved in biomineralization (Shi et al. 2013). Tyrosinase oxidizes tyrosine, and this process is part of the formation of the periostracum (Nagai et al. 2007; Zhang et al. 2012a), an important protective agent of the shell which is vulnerable to reduced thickness and alterations in chemical composition under low pH (Rodolfo-Metalpa et al. 2010; Gazeau et al. 2013; Ramajo et al. 2015). Tyrosinase was also shown to be a critical component in larval shell formation and mitigated shell damage from OA in the Portuguese oyster (*C. angulata*, Yang et al. 2017). Furthermore, a study of adaptation of the mussel *M. galloprovincialis* to OA found an outlier SNP in tyrosinase tyr3 isoform (Bitter et al. 2019).

A SNP inducing a stop codon was found in the gene mucin-5AC-like at a higher frequency in juveniles from the acidified conditions than juveniles in control conditions; additionally, this gene was upregulated under OA stress in larvae. Depending on the location, a stop-gained SNP will either not be translated, or the mRNA will be translated into a mutant protein that can have altered function if the stop codon is in the penultimate or last exon of the gene (Coban-Akdemir et al. 2018). One of the functions of mucins is the formation of the nacreous shell layer (Marin et al. 2000), similar to perlucins and other C-type lectins. Mucins have also been upregulated in response to OA in corals (Moya et al. 2016) and mussels (Zhao et al. 2020). Two genes, carbonic anhydrase and aggrecan core protein-like, were upregulated in acidified larvae and have similar functions. Carbonic anhydrases are involved in regulating intracellular and extracellular concentrations of  $\text{CO}_2$ ,  $\text{H}^+$ , and  $\text{HCO}_3^-$ , are important acid–base regulators, and can help maintain intracellular ( $\text{pH}_i$ ) and extracellular ( $\text{pH}_e$ ) pH (Chegwidzen et al. 2000). In *C. gigas*, it was found that aggrecan core proteins were involved in the calcification and calcium binding processes during early larval development (Foulon et al. 2019). Larval *M. mercenaria* also upregulated aggrecan 1 under OA conditions (Schwaner et al. 2022a). A SNP inducing a stop codon was also found in a gene with von Willebrand factor A domain with a higher frequency in juveniles in the acidified condition. The von Willebrand factor A domain is a common domain found in molluscan shell proteins (Rajan and Vengatesen 2020) and has been identified as a constituent of the basic tool kit for the biomineralization of the calcium carbonate molluscan shell (Arivalagan et al. 2017). Sydney rock oysters preconditioned to OA, which performed better under OA, showed high expression levels of von Willebrand factor D (Goncalves et al. 2017).

Only SNPs that were enriched in juvenile survivors of OA have been discussed; however, SNPs depleted under acidified conditions were identified. The optimal genotypes under normal conditions may not be the same genotype that would improve fitness under acidification. If a SNP caused an adverse change in gene function or caused a nonfunctional protein, it could have impacted the survival under OA conditions, which would not be reflected under normal conditions and could have been selected against. One such example can be found in the gene extensin-like, which codes for a skeletal matrix protein related to calcification (Shimizu et al. 2019), and contained a stop-gained SNP. The SNP in extensin-like was predicted as “Deleterious” by PROVEAN. If the SNP in extensin-like caused a change to protein function or a nonfunctional protein, it did not appear to adversely impact survivorship in control conditions, but it may have lowered fitness under acidification.

Interestingly, many of the genes identified in this study contained domains found in molluscan shell proteins such

as von Willebrand factor A, mucin, tyrosinase, epidermal growth factor, carbonic anhydrase, and C-type lectin. Many conserved domains found in molluscan shell proteins have other functions that are not related to shell formation and are considered “co-opted” for shell formation (Kocot et al. 2016; Aguilera et al. 2017; Rajan and Vengatesen 2020).

Rajan and Vengatesen (2020) recommended conducting research to look at genetic changes in molluscan biomineralization under ocean acidification to fill a gap in the literature. The research presented here highlights the importance of key biomineralization genes in eastern oyster response to OA and suggests important physiological changes under acidified conditions (Fig. 5).

### Hemocyte Function

Hemocytes, in both hemolymph and extrapallial fluid, play an important role in biomineralization as they supply crystalline  $\text{CaCO}_3$  for shell formation (Mount et al. 2004). Studies have demonstrated that exposure to OA decreases hemocyte viability (Cao et al. 2018), alters hemocyte function (Su et al. 2018), and causes an outflow of  $\text{Ca}^{2+}$  from hemocytes to hemolymph, which can impair the biomineralization process (Li et al. 2015). A SNP leading to a missense was found in the gene ankyrin-1-like at a higher frequency in the juvenile survivors of OA compared to the controls. Ankyrin-1-like plays key roles in ion channel activity and hemocyte function. It is part of the TRP family of ion channels that acts as a  $\text{Ca}^{2+}$  permeable cation channel (Nilius et al. 2012) and was shown to play an important role in the functioning of hemocytes in the pearl oyster (Wei et al. 2017). Another missense SNP was found in the isoforms of protein draper-like at a higher frequency in the juveniles from the acidified condition compared to the controls, and its expression was also upregulated in larvae under acidified conditions. The draper gene plays a part in hemocyte function in the fruit fly (*Drosophila melanogaster*, Manaka et al. 2004) and hemocyte aggregation in the mosquito (*Anopheles gambiae*, Sigle and Hillyer 2018). In *Drosophila*, draper-mediated phagocytosis was linked to  $\text{Ca}^{2+}$  homeostasis (Cuttell et al. 2008). OA can decrease  $\text{Ca}^{2+}$  content of hemocytes (Li et al. 2015), which may alter biomineralization processes.

### Cytoskeleton, Extracellular Matrix, and Cell Matrix Adhesion

In molecular biology, the term “skeletons” refers to cytoskeleton, extracellular matrix, and cell adhesion which make up an important network (Shen et al. 2018). Several studies show differential expression of skeletal genes induced by OA (Tomanek et al. 2011; Timmins-Schiffman et al. 2014; Goncalves et al. 2016; Li et al. 2016; Zhao et al. 2020) and higher frequencies of SNPs in related genes (Pespeni et al. 2013). One hypothesis is that high  $p\text{CO}_2$  causes oxidative

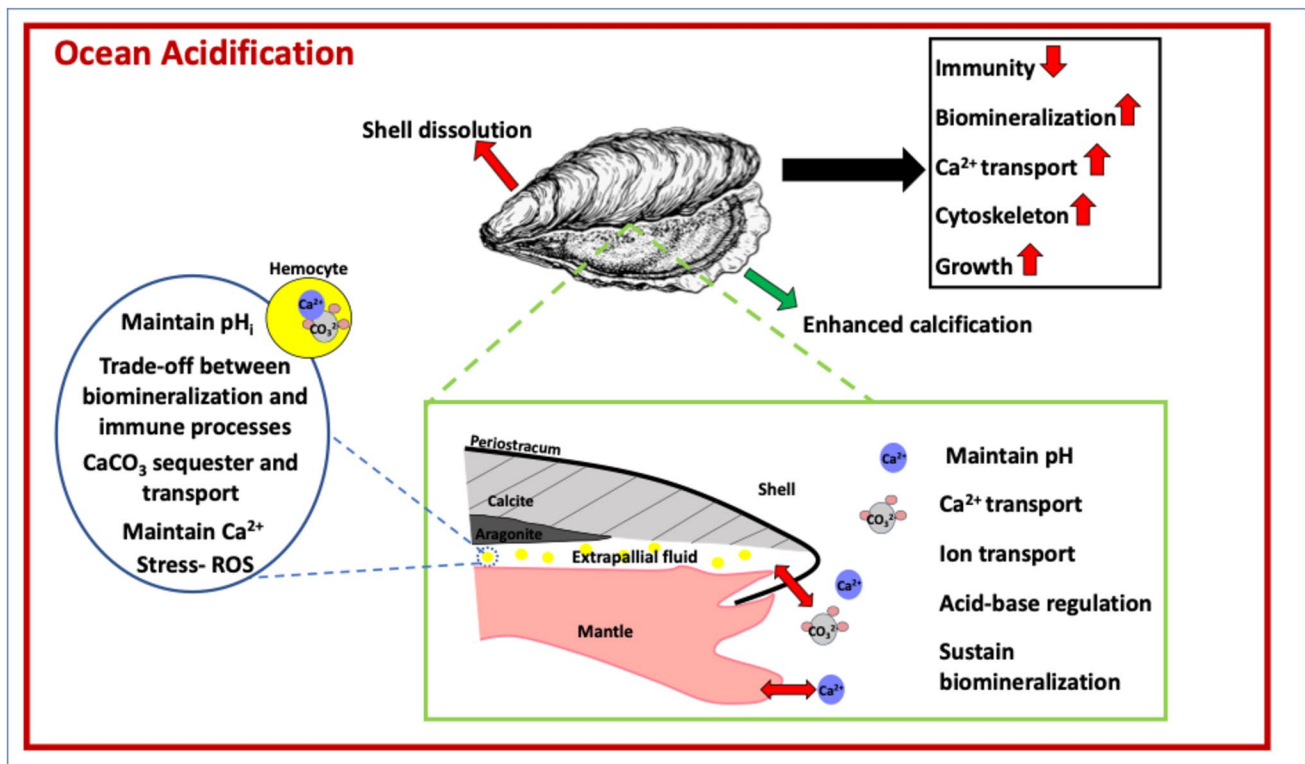


**Fig. 5** Schematic illustration of the physiological and molecular responses of oysters to OA. DEGs and genes with SNPs enriched in survivors of OA were identified and revealed processes impacted by

acidification. The specific genes involved in the highlighted processes are listed in Table 1 and are further addressed in the discussion

stress and cellular acidosis, leading the organisms to upregulate these genes to repair damage to the cytoskeleton (Tomanek et al. 2011). In addition, the extracellular matrix plays a role in shell formation (Dyachuk 2018) and mediates the nucleation, orientation, and growth of  $\text{CaCO}_3$  crystals (Suzuki and Nagasawa 2013), which would be constrained under OA.

Here, SNPs were found in kinesin, inducing a stop codon and has a higher frequency in the juvenile survivors of OA compared to the controls. Kinesin functions in cytoskeletal organization (Ronza et al. 2018), and the kinesin-1-complex was identified as one of the top ten upregulated GO terms in a study of the coral (*Lophelia pertusa*) under low pH (Glazier et al. 2020). Fibrillin-1-like contained a SNP inducing a stop codon, which was enriched in acidified juveniles compared to controls. Fibrillin is an extracellular matrix protein important for larval oyster development (Dyachuk 2018), and fibrillin-1-like was upregulated by *C. gigas* in response to OA (Wang et al. 2020). Cell adhesion molecules found in our study included cadherin EGF LAG seven-pass G-type receptor 3-like, which contained a synonymous SNP, was enriched in acidified juveniles compared to controls, and was upregulated in juvenile oysters under OA. A stop-gained SNP was found

enriched in *M. mercenaria* juveniles under OA conditions in the gene cadherin EGF LAG seven pass G type receptor 1 (Schwaner et al. 2022a). Genes with cadherin domains were upregulated in response to OA exposure in *C. gigas* (Timmins-Schiffman et al. 2014; Wang et al. 2020), and alleles of cadherin genes were unique to eastern oyster larvae that survived acidification stress (Barbosa 2020).

A SNP inducing a stop codon in dynein beta chain 2C flagellar outer-arm-like was depleted in acidified juveniles. The SNP was deemed “Deleterious” which could possibly explain why it appeared to be selected against in the acidified juveniles. Similarly, only control juveniles had a SNP in myosin-10-like which induced a stop codon and was predicted as “Deleterious.” *C. gigas* upregulates myosin heavy chain 95F and dynein heavy chain 3 under OA (Timmins-Schiffman et al. 2014). Both myosin and dynein have been shown to be involved in cell adhesion and cytoskeleton and extracellular matrix remodeling (Shen et al. 2018). Juvenile controls were enriched with the stop-gained SNP in proto-cadherin gamma-B4-like, and this variant was not detected in any of the acidified juveniles and was also identified as being putatively under selection and “Deleterious.” Proper functioning of the skeletal network appears to be important for resilience to OA in the eastern oyster.



## Immune and Stress Response

Bivalves often display alterations in their innate immune system under environmental stress, and previous studies, including our own work (Schwaner et al. 2020), showed that immunity in marine bivalves is sensitive to altered carbonate chemistry (Bibby et al. 2008; Liu et al. 2016; Wang et al. 2016; Castillo et al. 2017). High  $p\text{CO}_2$  can cause oxidative stress by increasing reactive oxygen species production (Tomanek et al. 2011), which can lead to an increase of apoptosis of hemocytes and alter cytoskeleton mediated engulfment of foreign particles (Su et al. 2018). G2 and S phase-expressed protein 1-like contained a SNP causing a missense and was enriched in juvenile survivors of OA compared to controls. This protein is in the FoxO signaling pathway, a family of transcription factors involved in apoptosis, cell-cycle control, and oxidative stress resistance in fish (Cai et al. 2020). Similarly, lactose-binding lectin 1–2 like (Burgos-Aceves and Faggio 2017; Zhang et al. 2020), antistasin-like (Nikapitiya et al. 2010), and baculoviral IAP repeat-containing protein 2-like (Pauletto et al. 2014) contribute to immunity in bivalves. All of these genes had SNPs inducing a stop codon and were enriched in acidified conditions.

Heat shock proteins (HSP) are partly responsible for the physiological plasticity of bivalves and have been recognized to contribute to the ability of these animals to survive in heterogeneous environments (Fabbri et al. 2008). Upregulation of HSPs has been found under OA stress in corals (Moya et al. 2015) and bivalves (Goncalves et al. 2017), while HSPs have been shown to be downregulated in urchins (Todgham and Hofmann 2009). Bitter et al. (2019) also found an outlier SNP under low pH in HSP70. In our study, one HSP was upregulated in acidified larvae; however, eight HSP were downregulated. *M. mercenaria* post-set juveniles downregulated HSPs under OA stress (Schwaner et al. 2022a). An outlier SNP inducing a stop codon was also found in tetratricopeptide repeat protein 37-like, enriched in juveniles from the acidified condition. Tetratricopeptide repeat protein is an adapter protein that assembles HSP 70 and 90 into a multi-chaperone complex (Scheufler et al. 2000).

HSP70, although initially upregulated under OA in the echinoderm *Asterias rubens*, returned to normal levels after long-term exposure suggesting it is too energetically expensive to over-express HSPs for extended periods (Hernroth et al. 2011). Other studies demonstrated that OA inhibits expression of HSPs and immune effectors, such as the downregulation of defensin, HSP70, and glutathione peroxidase after 28 days of exposure to  $\text{CO}_2$  in *C. gigas* (Wang et al. 2016). In this study, big defensin-like, peroxidase-like, and heat shock proteins 70 kDa protein 12A-like and 12B-like were downregulated in response to OA. The downregulation of HSPs and peroxidase could indicate a lowered ability to

defend against OA stress at the cellular level. The downregulation of stress and immune-related genes under acidified conditions could indicate physiological costs of exposure to OA (Table 1). Previous studies showed an increased susceptibility to pathogens in oysters and clams raised in acidified conditions (Schwaner et al. 2020) as well as in other bivalves (Liu et al. 2016; Cao et al. 2018; Su et al. 2018). The lectin fucolectin was downregulated in juveniles in response to OA, supporting results found in the marine worm (*Platynereis dumerilii*) submitted to low pH stress (Wage et al. 2016). Lectins are important pathogen recognition proteins (Patnaik et al. 2016; Saco et al. 2020), and ficolins are components of the lectin complement pathway. Ficolin-1-like and ficolin-2-like (Endo et al. 2007; Tanio et al. 2007) were downregulated in juvenile oysters under acidification. Genes related to the toll-like receptor pathway were also depressed in larval and juvenile oysters. Similarly, the blood clam (*Tegillarca granosa*) decreases expression of toll-like receptors under OA, likely contributing to their weakened immune response (Liu et al. 2016). Continuous upregulation of stress and immune-related genes under OA is costly and might increase susceptibility to disease until there is a selection of resilient oysters.

## Growth and Development

In a study of genetic differences between populations of sea urchins cultured under different  $p\text{CO}_2$  treatments, significant genetic changes were found in genes involved in growth (Pespeni et al. 2013). OA causes differences in morphology, reduces size, and alters development in many organisms (Talmage and Gobler 2010; Barros et al. 2013; Schwaner et al. 2020). For example, low pH has detrimental effects on the calcification process during embryogenesis in *C. gigas* (Kurihara et al. 2007). In this study, cholecystokinin receptor type A-like was found to contain a SNP causing a missense and had higher frequency in juveniles from acidified conditions compared to juveniles from control. This gene has been detected in governing embryonic development of the channeled apple snail (*Pomacea canaliculata*, Xiong et al. 2018). Embryonic morphogenesis was an over-represented GO term for larvae submitted to pH stress. The gene cilia-and-flagella-associated protein might also play a role in larval development, particularly in the formation of the velum organ (Trigg et al. 2020). *M. galloprovincialis* larvae exposed to low pH have protruding velum, indicating abnormal tissue development or inability to retract that organ (Kapsenberg et al. 2018). The velum organ and ciliary movement is important for larval feeding (Gallager 1988), and studies have shown that increased feeding can offset impacts of OA (Hettinger et al. 2013; Thomsen et al. 2013; Ramajo et al. 2016). Cilia-and-flagella-associated protein 54-like was found to have a SNP causing a missense with a

higher frequency in survivors of OA compared to the controls. Growth factors play critical roles in regulating growth, cell differentiation, and embryogenesis (LeLong et al. 2001). Multiple epidermal growth factor (EGF)-like domains protein 6 contained a SNP inducing a stop-codon and it had higher frequencies in acidified juveniles compared to controls. Multiple epidermal growth factor-like domains protein 10 and 11 expression was also upregulated in larvae and juveniles from acidified conditions. Sydney rock oysters that performed better under OA, due to preconditioning, upregulated EGF (Goncalves et al. 2017). While EGFs are known to be involved in development and growth, EGFs have been found in shell matrix proteins and might also be important for bivalve biomineralization (Marie et al. 2012; Rajan and Vengatesen 2020).

The larval oysters in the acidified conditions were significantly smaller than controls, but by the juvenile stage, there were no differences in size. The smaller larvae appeared to die during larval development, leading to a cohort of larger individuals that persisted to the juvenile stage in the acidified conditions. These juveniles contained SNPs in genes that are related to growth and development.

Although this study demonstrates genetic variation between oysters raised under acidified and control conditions, it remains unclear if one SNP in one locus actually modifies global expression or if compensatory mechanisms exist to alleviate the potential negative effects of detrimental variants. Further investigations using gene knockdown methods (e.g., RNAi) are underway to validate the role of candidate genes in resilience to OA.

Layton and Bradbury (2022) called for researchers to broaden their approach and utilize multi-omic methods to predict the response of marine organisms to climate change. This is one of the first studies in eastern oyster to investigate transcriptional modulation and genetic polymorphism to probe resilience to OA at the molecular level. Results support both adaptation potential through the selection of animals with specific resilience-associated SNPs and the capacity for oysters to regulate gene expression to mitigate the effects of OA. These findings support that oysters have an adaptive capacity to withstand mild OA, and that selective breeding might be a potential solution for aquaculture and restoration programs. It remains however unclear if a limited number of SNPs actually modify global gene expression or if compensatory mechanisms exist to alleviate the potential negative effects of detrimental variants. Similarly, the specific role of putative genes requires validation and investigations using RNAi are underway to validate the role of candidate genes in resilience to OA. While these findings spark hope that the eastern oyster can overcome OA stress through acclimation and adaptation, future experiments need to be conducted over multiple generations to confirm the long-term adaptation potential of this species.

**Supplementary Information** The online version contains supplementary material available at <https://doi.org/10.1007/s10126-023-10255-y>.

**Acknowledgements** The authors would like to thank Marty Byrnes and Rebecca Resner of the Great Atlantic Shellfish Hatchery for providing access to their hatchery and logistical support. We would also like to thank the Marine Animal Disease Laboratory intern Margot Eckstein for help with bivalve maintenance. In addition, we would also like to thank Dr. Christopher Gobler and Andrew Lundstrom for processing DIC samples.

**Author Contribution** Caroline Schwaner contributed to formal analysis, investigation, methodology, and writing the original draft. Sarah Farhat contributed to formal analysis and manuscript revisions. Isabelle Boutet and Arnaud Tanguy assisted with investigation and methodology. Michelle Barbosa helped with investigation. Denis Grouzdev assisted with formal analysis. Emmanuelle Pales Espinosa helped with methodology, manuscript revisions, and funding. Bassem Allam provided funding, assisted with investigation, conceptualization, project administration, and reviewing and editing.

**Funding** This research was funded by the New York Sea Grant (Projects R/XG-24 and R/XG-33 to Bassem Allam and Emmanuelle Pales Espinosa). Additional support was provided by the National Science Foundation (IOS 1656753) and the Atlantic States Marine Fisheries Commission (Contract 19–0802).

**Data Accessibility** Sequence reads are deposited in the SRA NCBI database and can be found under the BioProject ID PRJNA765289.

## Declarations

**Conflict of Interest** The authors declare no competing interests.

## References

- Aguilera F, McDougall C, Degnan BM (2017) Co-option and de novo gene evolution underlie molluscan shell diversity. *Mol Biol Evol* 34(4):779–792
- Alexa A, Rahnenfuhrer J (2020) topGO: Enrichment analysis for gene ontology. R package version 2.40.0
- Arivalagan J, Yarra T, Marie B, Sleight VA, Duvernois-Berthet E, Clark MS, Marie A, Berland S (2017) Insights from the shell proteome: biomineralization to adaptation. *Mol Biol Evol* 34:66–77
- Barbosa M (2020) Physiological and molecular traits associated with resilience to ocean acidification in *Crassostrea virginica*. State University of New York at Stony Brook (Doctoral dissertation)
- Barbosa M, Schwaner C, Pales Espinosa E, Allam B (2022) A transcriptomic analysis of phenotypic plasticity in *Crassostrea virginica* larvae under experimental acidification. *Genes* 13:1529. <https://doi.org/10.3390/genes13091529>
- Barret DH, Schluter D (2008) Adaptation from standing genetic variation. *Trends Ecol Evol* 23:38–44
- Barros P, Sobral P, Range P, Chicharo L, Matias D (2013) Effects of sea-water acidification on fertilization and larval development of the oyster *Crassostrea gigas*. *J Exp Mar Biol Ecol* 440:200–206
- Baumann H, Wallace RB, Tagliaferri T, Gobler CJ (2015) Large natural pH, CO<sub>2</sub>, and O<sub>2</sub> fluctuations in a temperate tidal salt marsh on diel, seasonal, and interannual time scales. *Estuaries Coasts* 38:220–231
- Bay RA, Palumbi SR (2014) Multilocus adaptation associated with heat resistance in reef-building corals. *Curr Biol* 24:2952–2956

- Beniash E, Ivanina A, Lieb NS, Kurochkin I, Sokolova IM (2010) Elevated level of carbon dioxide affects metabolism and shell formation in oysters *Crassostrea virginica*. *Mar Ecol Prog Ser* 419:95–108
- Bibby R, Widdicombe S, Parry H, Spicer J, Pipe R (2008) Effects of ocean acidification on the immune response of the blue mussel *Mytilus edulis*. *Aquat Biol* 2:67–74
- Bitter MC, Kapsenberg L, Gattuso JP, Pfister CA (2019) Standing genetic variation fuels rapid adaptation to ocean acidification. *Nat Commun* 10:5821. <https://doi.org/10.1038/s41467-019-13767-1>
- Bitter MC, Kapsenberg L, Silliman K, Gattuso JP, Pfister CA (2021) Magnitude and predictability of pH fluctuations shape plastic responses to ocean acidification. *Am Nat* 197:486–501
- Blank S, Arnoldi M, Khoshnavaz S, Treccani L, Kuntz M, Mann K, Grathwohl G, Fritz M (2003) The nacre protein perlucin nucleates growth of calcium carbonate crystals. *J Microsc* 212:280–291
- Boutet I, Monteiro HJA, Baudry L, Takeuchi T, Bonnivard E, Billoud B, Farhat S, Gonzales-Araya R, Salaun B, Andersen AC, Touleuc J, Lallier FH, Flot JF, Guiguelmoni N, Guo X, Li C, Allam B, Pales-Espinosa E, Hemmer-Hansen J, Moreau P, Marbouty M, Koszul R, Tanugy A (2022) Chromosomal assembly of the flat oyster (*Ostrea edulis* L.) genome as a new genetic resource for aquaculture. *Evol Appl*. <https://doi.org/10.1111/eva.13462>
- Burgos-Aceves MA, Faggio C (2017) An approach to the study of the immunity functions of bivalve hemocytes: physiology and molecular aspects. *Fish Shellfish Immunol* 67:513–517
- Calosi P, Rastrick SPS, Lombardi C, de Guzman HJ, Davidson L, Jahnke M, Giangrande A, Hardege JD, Schulze A, Spicer JL, Gambi MC (2013) Adaptation and acclimatization to ocean acidification in marine ectotherms: an in suite transplant experiment with polychaetes at a shallow CO<sub>2</sub> vent system. *Philos Trans R Soc B* 368:2012044. <https://doi.org/10.1098/rstb.2012.0444>
- Cai LS, Wang L, Song K, Lu KL, Zhang CX, Rahimnejad S (2020) Evaluation of protein requirement of spotted seabass (*Lateolabrax maculatus*) under two temperatures, and the liver transcriptome response to thermal stress. *Aquaculture* 516:734615
- Cao R, Wang Q, Yang D, Liu Y, Ran W, Qu Y, Wu H, Cong M, Li F, Ji C, Zhao J (2018) CO<sub>2</sub>-induced ocean acidification impairs the immune function of the Pacific oyster against *Vibrio splendidus* challenge: an integrated study from a cellular and proteomic perspective. *Sci Total Environ* 625:1574–1583. <https://doi.org/10.1016/j.scitotenv.2018.01.056>
- Carreiro-Silva M, Cerqueira T, Godinho A, Caetano M, Santos RS, Bettencourt R (2014) Molecular mechanisms underlying the physiological responses of the cold-water coral *Desmophyllum dianthus* to ocean acidification. *Coral Reefs* 33:465–476
- Castillo N, Saavedra LM, Vargas CA, Gallardo-Escarate C, Detree C (2017) Ocean acidification and pathogen exposure modulate the immune response of the edible mussel *Mytilus chilensis*. *Fish Shellfish Immunol* 70:149–155
- Chegwidden WR, Carter ND, Edwards YH (2000) *The carbonic anhydrases: new horizons*. Birkhäuser, Basel
- Choi Y, Sims GE, Murphy S, Miller JR, Chan AP (2012) Predicting the functional effect of amino acid substitutions and indels. *PLoS ONE* 7:e46688. <https://doi.org/10.1371/journal.pone.0046688>
- Coban-Akdemir Z, White JJ, Song X, Jhangiani SN, Faith JM, Gambin T, Bayram Y, Chinn IK, Karaca E, Punetha J, Poli C, Boerwinkle E, Shaw CA, Orange JS, Gibbs RA, Lappalainen T, Lupski JR, Carvalho CMB (2018) Identifying genes whose mutant transcripts cause dominant disease traits by potential gain-of-function alleles. *Am J Hum Genet* 103:171–187
- Cuttell L, Vaughan A, Silva E, Escaron CJ, Lavine M, Van Goethem E, Eid JP, Quirin M, Franc NC (2008) Undertaker, a Drosophila junctophilin, links draper-mediated phagocytosis and calcium homeostasis. *Cell* 135:524–534
- DeWit P, Palumbi SR (2013) Transcriptome-wide polymorphisms of red abalone (*Haliotis rufescens*) reveal patterns of gene flow and local adaptation. *Mol Ecol* 22:2884–2897
- De Wit P, Durland E, Ventura A, Langdon CJ (2018) Gene expression correlated with delay in shell formation in larval Pacific oysters (*Crassostrea gigas*) exposed to experimental ocean acidification provides insights into shell formation mechanisms. *BMC Genomics* 19:160. <https://doi.org/10.1186/s12864-018-4519-y>
- Dineshran R, Quan Q, Sharma R, Chandramouli K, Yalamanchili HK, Chu I, Thiyagarjan V (2015) Comparative and quantitative proteomics reveal the adaptive strategies of oyster larvae to ocean acidification. *Proteomics* 15:4120–4134
- Downey-Wall AM, Cameron LP, Ford BM, McNally EM, Venkataraman YR, Roberts SB, Ries JB, Lotterhos KE (2020) Ocean acidification induces subtle shifts in gene expression and DNA methylation in mantle tissue of the Eastern oyster (*Crassostrea virginica*). *Front Mar Sci* 7:566419. <https://doi.org/10.3389/fmars.2020.566419>
- Dyachuk V (2018) Extracellular matrix components in Bivalvia: shell and ECM components in development and adult tissues. *Fish Aqua J* 9:2. <https://doi.org/10.4172/2150-3508.1000248>
- Endo Y, Matsushita M, Fujita T (2007) Role of ficolin in innate immunity and its molecular basis. *Immunobiology* 212:371–379
- Evans TG, Chang F, Menge BA, Hofmann GE (2013) Transcriptomic responses to ocean acidification in larval sea urchins from a naturally variable pH environment. *Mol Ecol* 22:1609–1625
- Fabbri E, Valbonesi P, Franzellitti S (2008) HSP expression in bivalves *ISJ* 5:135–161
- Farhat S, Tanguy A, Pales Espinosa E, Guo X, Boutet I, Smolowitz R, Murphy D, Rivara GJ, Allam B (2020) Identification of variants associated with hard clam, *Mercenaria mercenaria*, resistance to quahog parasite unknown disease. *Genomics* 112:4887–4896
- Foll M, Gaggiotti OE (2008) A genome scan method to identify selected loci appropriate for both dominant and codominant markers: a Bayesian perspective. *Genetics* 180:977–993
- Foulon V, Boudry P, Artigaud S, Guerard F, Hellio C (2019) In silico analysis of the Pacific oyster (*Crassostrea gigas*) transcriptome over developmental stages reveals candidate genes for larval settlement. *Int J Mol Sci* 20:197. <https://doi.org/10.3390/ijms20010197>
- Frieder CA, Applebaum SL, Pan TCF, Hedgecock D, Manahan DT (2017) Metabolic cost of calcification in bivalve larvae under experimental ocean acidification. *ICES J Mar Sci* 74:941–954
- Gallager SM (1988) Visual observation of particle manipulation during feeding in larvae of a bivalve mollusc. *Bull Mar Sci* 43:344–365
- Gazeau F, Quiblier C, Jansen JM, Gattuso JP, Middleburg JJ, Heip CHR (2007) Impact of elevated CO<sub>2</sub> on shellfish calcification. *Geophys Res Lett* 34:L07603. <https://doi.org/10.1029/2006GL028554>
- Gazeau F, Gattuso JP, Dawber C, Pronker AE, Peene F, Peene J, Heip CHR, Middleburg JJ (2010) Effect of ocean acidification on the early life stages of the blue mussel *Mytilus edulis*. *Biogeosciences* 7:2051–2060
- Gazeau F, Parker LM, Comeau S, Gattuso JP, O'Connor WA, Martin S, Pörtner HO, Ross PM (2013) Impacts of ocean acidification on marine shelled molluscs. *Mar Biol* 160:2207–2245
- Glazier A, Herrera S, Weininger A, Kurman M, Gomez CE, Cordes E (2020) Regulation of ion transport and energy metabolism enables certain coral genotypes to maintain calcification under experimental ocean acidification. *Mol Ecol* 29:1657–1673
- Gobler CJ, Talmage SC (2014) Physiological response and resilience of early life-stage Eastern oysters (*Crassostrea virginica*) to past, present and future ocean acidification. *Conserv Physiol* 2:cou004. <https://doi.org/10.1093/conphys/cou004>

- Goncalves P, Anderson K, Thompson EL, Melwani A, Parker L, Ross PM, Raftos DA (2016) Rapid transcriptional acclimation following transgenerational exposure of oysters to ocean acidification. *Mol Ecol* 25:4836–4849
- Goncalves P, Jones DB, Thompson EL, Parker LM, Ross PM, Raftos DA (2017) Transcriptomic profiling of adaptive responses to ocean acidification. *Mol Ecol* 26:5974–5988
- Griffiths JS, Pan TF, Kelly MW (2019) Differential responses to ocean acidification between populations of *Balanophyllia elegans* corals from high and low upwelling environments. *Mol Ecol* 28:2715–2730
- Grunwald NJ, Kamvar ZN, Everhart SE, Tabima JF, Kanus BJ (2017) Population genetics and genomics in R. Retrieved from [https://grunwaldlab.github.io/Population\\_Genetics\\_in\\_R/](https://grunwaldlab.github.io/Population_Genetics_in_R/). Accessed 30 Jul 2019
- Helm MM, Bourne N, Lovatelli A (2004) Hatchery culture of bivalves: a practical manual. Food and Agriculture Organization of the United Nations, Rome
- Hermisson J, Pennings PS (2005) Soft sweeps: molecular population genetics of adaptation from standing genetic variation. *Genetics* 169:2335–2352
- Hernroth B, Baden S, Thorndyke M, Dupont S (2011) Immune suppression of the echinoderm *Asterias rubens* (L.) following long-term ocean acidification. *Aquat* 103:222–224
- Hess JE, Campbell NR, Close DA, Docker MF, Narum SR (2013) Population genomics of Pacific lamprey: adaptive variation in a highly dispersive species. *Mol Ecol* 22:2898–2916
- Hettinger A, Sanford E, Hill TM, Hosfelt JD, Russell AD, Gaylord B (2013) The influence of food supply on the response of *Olympia* oyster larvae to ocean acidification. *Biogeosciences* 10:6629–6638
- Hüning AK, Melzner F, Thomsen J, Gutowska MA, Krämer L, Frickenhaus S, Rosenstiel P, Pörtner HO, Philipp EER, Lucassen M (2013) Impacts of seawater acidification on mantle gene expression patterns of the Baltic Sea blue mussel: implications for shell formation and energy metabolism. *Mar Biol* 160:1845–1861
- Hunt S (1987) Amino acid compositions of periostracal proteins from molluscs living in the vicinity of deep sea hydrothermal vents: an unusual methionine-rich structural protein. *Comp Biochem Phys* 88:1013–1021
- Hunt R, Sauna ZE, Ambudkar SV, Gottesman MM, Kimchi-Sarfaty C (2009) Silent (synonymous) SNPs: should we care about them? Single nucleotide polymorphisms: methods and protocols. Humana Press, Totowa, NJ, pp 23–39
- Johnson KM, Hofmann GE (2017) Transcriptomic response of the Antarctic pteropod *Limacina helicina antarctica* to ocean acidification. *BMC Genomics* 18(1):1–16
- Jong MJ, Jong JF, Hoelzel AR, Janke A (2021) SambaR: an R package for fast, easy and reproducible population-genetic analyses of biallelic SNP datasets. *Mol Ecol Resour* 21:1369–1379
- Kapsenberg L, Miglioli A, Bitter MC, Tambutte E, Dumollard R, Gattuso JP (2018) Ocean pH fluctuations affect mussel larvae at key developmental transitions. *Proc Royal Soc B* 285:20182381. <https://doi.org/10.1098/rspb.2018.2381>
- Kelly MW, Padilla-Gamiño JL, Hofmann GE (2013) Natural variation and the capacity to adapt to ocean acidification in the keystone sea urchin *Strongylocentrotus purpuratus*. *Glob Change Biol* 19:2536–2546
- Kim D, Paggi JM, Park C, Bennett C, Salzberg SL (2019) Graph-based genome alignment and genotyping with HISAT2 and HISAT-genotype. *Nat Biotechnol* 37:907–915
- Kocot KM, Aguilera F, McDougall C, Jackson DJ, Degnan BM (2016) Sea shell diversity and rapidly evolving secretomes: insights into the evolution of biomineralization. *Front Zool* 13:23
- Kurihara H, Kato S, Ishimatsu A (2007) Effects of increased seawater pCO<sub>2</sub> on early development of the oyster *Crassostrea gigas*. *Aquat Biol* 1:91–98
- Larmuseau MHD, Vancampenhout K, Raeymaekers JAM, Van Houdt JKJ, Volckaert FAM (2010) Differential modes of selection on the rhodopsin gene in coastal Baltic and North Sea populations of the sand goby, *Pomatoschistus minutus*. *Mol Ecol* 19:2256–2268
- Layton KK, Bradbury IR (2022) Harnessing the power of multi-omics data for predicting climate change response. *J Anim Ecol* 91(6):1064–1072
- Lelong C, Mathieu M, Favrel P (2001) Structure and expression of mGDF, a new member of the transforming growth factor-B superfamily in the bivalve mollusc *Crassostrea gigas*. *Eur J Biochem* 267:3986–3993
- Li S, Liu Y, Liu C, Huang J, Zheng G, Xie L, Zhang R (2015) Morphology and classification of hemocytes in *Pinctada fucata* and their responses to ocean acidification and warming. *Fish Shellfish Immunol* 45:194–202
- Li S, Liu C, Huang J, Liu Y, Zhang S, Zheng G, Xie L, Zhang R (2016) Transcriptome and biomineralization responses of the pearl oyster *Pinctada fucata* to elevated CO<sub>2</sub> and temperature. *Sci Rep* 6:18943. <https://doi.org/10.1038/srep18943>
- Liu S, Shi W, Guo C, Zhao X, Han Y, Peng C, Chai X, Liu G (2016) Ocean acidification weakens the immune response of blood clam through hampering the NF-kappa  $\beta$  and toll-like receptor pathways. *Fish Shellfish Immunol* 54:322–327
- Loosanoff VL (1966) Time and intensity of setting of the oyster, *Crassostrea virginica*, in Long Island Sound. *Biol Bull* 130:211–227
- Lopez-Landavery EA, Carpizo-Ituarte EJ, Perez-Carrasco L, Diaz F, De le Cruz FL, Garcia-Esquivel Z, Hernandez-Ayon JM, Galindo-Sanchez CE (2021) Acidification stress effect on umbonate veliger larval development in *panopea globosa*. *Mar Poll Bull* 163:111945
- Lowenstam HA, Weiner S (1989) On biomineralization. Oxford University Press, Oxford
- Luu K, Bazin E, Blum MGB (2017) pcadapt: a R package to perform genome scans for selection based on principal component analysis. *Mol Ecol Resour* 1:67–77
- Maas AE, Lawson G, Tarrant AM (2015) Transcriptome-wide analysis of the response of the thecosome pteropod *clio* pyramidata to short-term CO<sub>2</sub> exposure. *Comp Biochem Physiol Part d Genom Proteom* 16:1–9
- Manaka J, Kuraishi T, Shiratsuchi A, Nakai Y, Higashida H, Henson P, Nakanishi Y (2004) Draper-mediated and phosphatidylserine-independent phagocytosis of apoptotic cells by *Drosophila* hemocytes/macrophages. *J Biol Chem* 279:48466–48476
- Marie B, Joubert C, Tayalé A, Zanella-Cléon BC, Piquemal D, Cochenne-Laureau N, Marin F, Gueguen Y, Montagnani C (2012) Different secretory repertoires control the biomineralization processes of prism and nacre deposition of the pearl oyster shell. *PNAS* 109:20986–20991
- Marie B, Arivalagan J, Matheron L, Bolbach G, Berland S, Marie A, Marin F (2017) Deep conservation of bivalve nacre proteins highlighted by shell matrix proteomics of the Unionoida *Elliptio complanata* and *Villosa lienosa*. *J R Soc Interface* 14:20160846. <https://doi.org/10.1098/rsif.2016.0846>
- Marin F, Corstjens P, Gaulejac BD, de Vrind-De JE, Westbroek P (2000) Mucins and molluscan calcification molecular characterization of mucoperlin, a novel mucin-like protein from the nacreous shell layer of the fan mussel *Pinna nobilis* (*Bivalvia, pteriomorpha*). *J Biol Chem* 275:20667–20675
- Martin S, Richier S, Pedrotti ML, Dupont S, Castejon C, Gerakis Y, Kerros M, Oberhansli F, Teyssie J, Jeffree R, Gattuso JP (2011) Early development and molecular plasticity in the Mediterranean sea urchin *Paracentrotus lividus* exposed to CO<sub>2</sub>-driven acidification. *J Exp Biol* 214(8):1357–1368
- Metzger DC (2012) Characterizing the effects of ocean acidification in larval and juvenile Manila clam, *Ruditapes philippinarum*, using a transcriptomic approach. University of Washington, Washington, DC, USA (Master's Thesis)

- Millero FJ (2010) Carbonate constants for estuarine waters. *Mar Freshw Res* 62:139–142
- Mount AS, Wheeler AP, Paradkar RP, Snider D (2004) Hemocyte-mediate shell mineralization in the eastern oyster. *Science* 304:297–300
- Moya A, Huisman L, Ball E, Hayward D, Grasso L, Chua C, Woo HN, Gattuso JP, Foret S, Miller DJ (2012) Whole transcriptome analysis of the coral *Acropora millepora* reveals complex responses to CO<sub>2</sub> driven acidification during the initiation of calcification. *Mol Ecol* 21:2440–2454
- Moya A, Huisman L, Foret S, Gattuso JP, Hayward DC, Ball EE, Miller DJ (2015) Rapid acclimation of juvenile corals to CO<sub>2</sub>-mediated acidification by upregulation of heat shock protein and Bcl-2 genes. *Mol Ecol* 24(2):438–452
- Moya A, Howes EL, Lacoue-Labarthe T, Foret S, Hanna B, Medina M, Munday PL, Ong JS, Yeyssie JL, Torda G, Watson SA, Miller DJ, Bijma J, Gattuso JP (2016) Near-future pH conditions severely impact calcification, metabolism, and the nervous system in the pteropod *Heliconoides inflatus*. *Glob Change Biol* 22:3888–3900
- Nagai K, Yano M, Morimoto K, Miyamoto H (2007) Tyrosinase localization in mollusc shells. *Comp. Biochem. Physiol. B. Biochem Mol Biol* 146:207–214
- Nikapitiya C, De Zoysa M, Oh C, Lee Y, Ekanayake PM, Whang I, Choi CY, Lee JS, Lee J (2010) Disk abalone (*Haliotis discus discus*) expresses a novel antistatin-like serine protease inhibitor: molecular cloning and immune response against bacterial infection. *Fish Shellfish Immunol* 28:661–671
- Nilius B, Appendino G, Owsianik G (2012) The transient receptor potential channel TRPA1: from gene to pathophysiology. *Pflug Arch Eur J Phy* 464:425–458
- O'Donnell MJ, Todgham AE, Sewell MA, Hammond LM, Ruggiero K, Fanguie NA, Zippay ML, Hofmann GE (2010) Ocean acidification alters skeletogenesis and gene expression in larval sea urchins. *Mar Ecol Prog Ser* 398:157–171
- Palumbi S, Oliver T (2006) Genetic evidence of dispersal limitation and local adaptation in Samoan reef corals: report on ongoing research: March 2006
- Pan TCF, Applebaum SL, Manahan DT (2015) Experimental ocean acidification alters the allocation of metabolic energy. *Proc Natl Acad Sci* 112:4696–4701. <https://doi.org/10.1073/pnas.1416967112>
- Parker LM, Ross PM, O'Connor WA (2011) Populations of the Sydney rock oyster, *Saccostrea glomerata*, vary in response to ocean acidification. *Mar Biol* 158:689–697
- Patnaik BB, Wang TH, Kang SW, Hwang HJ, Park SY, Park EB, Chung JM, Song DK, Kim C, Kim S, Lee JS, Han YS, Park HS, Lee YS (2016) Sequencing, de novo assembly, and annotation of the transcriptome of the endangered freshwater pearl bivalve, *Cristaria plicata*, provides novel insights into functional genes and marker discovery. *PLoS ONE* 11:e0148622. <https://doi.org/10.1371/journal.pone.0148622>
- Pauletto M, Milan M, Moreira R, Novoa B, Figueras A, Babbucci M, Patarnello T, Bargelloni L (2014) Deep transcriptome sequencing of *Pecten maximus* hemocytes: a genomic resource for bivalve immunology. *Fish and Shellfish Immunol* 37:154–165
- Pespeni MH, Sanford E, Gaylord B, Hill TM, Hosflet JD, Jaris HK, LaVigne M, Lenz EA, Russell AD, Young MK, Palumbi SR (2013) Evolutionary change during experimental ocean acidification. *Proc Natl Acad Sci USA* 110:6937–6942
- Peterson BK, Weber JN, Kay EH, Fisher HS, Hoekstra HE (2012) Double digest RADseq: an inexpensive method for de novo SNP discovery and genotyping in model and non-model species. *PLoS ONE* 7:e37135. <https://doi.org/10.1371/journal.pone.0037135>
- Powell D, Subramanian S, Suwansaard S, Zhao M, O'Connor W, Raftos D, Elizur A (2018) The genome of the oyster *Saccostrea* offers insight into the environmental resilience of bivalves. *DNA Res* 25:655–665
- Putri GH, Anders S, Pyl PT, Pimada JE, Zanini F (2022) Analyzing high-throughput sequencing data in Python with HTSeq 2.0. *Bioinformatics*. <https://doi.org/10.1093/bioinformatics/btac166>
- Rajan KC, Vengatesen T (2020) Molecular adaptation of molluscan biomineralization to high CO<sub>2</sub> oceans- the known and the unknown. *Mar Environ Res* 155:104883
- Rajan KC, Meng Y, Roberts SB, Vengatesen T (2021) Oyster biomineralization under ocean acidification: from genes to shell. *Glob Change Biol* 27:3779–3797
- Ramajo L, Marba N, Prado L, Peron S, Lardies M, Rodriguez-Navarero VCA, Lagos NA, Duarte CM (2015) Biomineralization changes with food supply confer juvenile scallops (*Agropecten purpuratus*) resistance to ocean acidification. *Glob Change Biol* 22:2025–2037
- Ramajo L, Perez-Leon E, Hendriks IE, Marba N, Krause-Jensen D, Sejr MK, Blicher ME, Lagos N, Olsen Y, Duarte CM (2016) Food supply confers calcifiers resistance to ocean acidification. *Sci Rep* 6:19374. <https://doi.org/10.10138/srep19374>
- Reusch TBH (2013) Climate change in the oceans: evolutionary versus phenotypically plastic responses of marine animals and plants. *Evo App* 7:104–122
- Rochette NC, Rivera-Colón AG, Catchen JM (2019) Stacks 2: analytical methods for paired-end sequencing improve RADseq-based population genomics. *Mol Ecol* 28(21):4737–4754. <https://doi.org/10.1111/mec.15253>
- Robinson MD, McCarthy DJ, Smyth GK (2010) edgeR: a bioconductor package for differential expression analysis of digital gene expression data. *Bioinformatics* 26:139–140
- Rodolfo-Metalpa R, Lombardi C, Cocito S, Hall-Spencer JM, Gambi MC (2010) Effects of ocean acidification and high temperatures on the bryozoan *Myriapora truncata* at natural CO<sub>2</sub> vents. *Mar Ecol* 31:447–456
- Ronza P, Cao A, Robledo D, Gomez-Tato A, Alvarez-Dios JA, Hasanuzzaman AFM, Quiroga MI, Villalba A, Pardo BG, Martinez P (2018) Long-term affected flat oyster (*Ostrea edulis*) haemocytes show differential gene expression profiles from naive oysters in response to *Bonamia ostreae*. *Genomics* 110:390–398
- Saba GK, Goldsmith KA, Cooley SR, Grosse D, Meseck SL (2019) Recommended priorities for research on ecological impacts of ocean and coastal acidification in the U.S. mid-Atlantic. *Estuar Coast Shelf Sci* 225:106188. <https://doi.org/10.1016/j.ecss.2019.04.022>
- Saco A, Rey-Campos M, Novoa B, Figueras A (2020) Transcriptomic response of mussel gills after a *Vibrio splendidus* infection demonstrates their role in the immune response. *Front Immunol* 11:615580. <https://doi.org/10.3389/fimmu.2020.615580>
- Scheufler C, Brinker A, Bourenkov G, Pegoraro S, Moroder L, Bartunik H (2000) Structure of TPR domain-peptide complexes: critical elements in the assembly of the HSP70-HSP90 multichaperone machine. *Cell* 101:199–210
- Schluter L, Lohbeck KT, Gutowska MA, Groger JP, Riebesell U, Reusch T (2014) Adaptation of a globally important coccolithophore to ocean warming and acidification. *Nat Clim Change* 4:1024–1030
- Schwaneer C, Barbosa M, Connors P, Park TJ, de Silva D, Griffith A, Gobbler CJ, Pales Espinosa E, Allam B (2020) Experimental acidification increases susceptibility of *mercenaria mercenaria* to infection by *vibrio* species. *Mar Environ Res* 154:104872. <https://doi.org/10.1016/j.marenvres.2019.104872>
- Schwaneer C, Farhat S, Barbosa M, Boutet I, Tanguy A, Pales Espinosa E, Allam B (2022a) Molecular features associated with resilience to ocean acidification in the northern quahog, *Mercenaria mercenaria*. *Mar Biotechnol*. <https://doi.org/10.1007/s10126-022-10183>
- Schwaneer C, Farhat S, Haley J, Pales Espinosa E, Allam B (2022b) Proteomic and transcriptomic responses enable clams to correct the pH of calcifying fluids and sustain biomineralization in acidified environments. *Int J Mol Sci* 23:16066. <https://doi.org/10.3390/ijms232416066>

- Schwamer C, Pales Espinosa E, Allam B (2023) RNAi silencing of the biomineralization gene perlucin impairs oyster ability to cope with ocean acidification. *Int J Mol Sci* 24:3661. <https://doi.org/10.3390/ijms24043661>
- Shen M, Di G, Li M, Fu J, Dai Q, Miao X, Huang M, You W, Ke C (2018) Proteomics studies on three larval stages of development and metamorphosis of *Babylonia areolata*. *Sci Rep* 8:6269. <https://doi.org/10.1093/gbe/evy242>
- Shi Y, Yu C, Gu Z, Zhan X, Wang Y, Wang A (2013) Characterization of the pearl oyster (*Pinctada martensii*) mantle transcriptome unravels biomineralization genes. *Mar Biotechnol* 15:175–187
- Shimizu K, Kimura K, Isowa Y, Oshima K, Ishikawa M, Kagi H, Kito K, Hattori M, Chiba S, Endo K (2019) Insights into the evolution of shells and love darts of land snails revealed from their matrix proteins. *Genome Biol Evol* 11:380–397
- Sigle LT, Hillyer JF (2018) Eater and draper are involved in the peritostial haemocyte immune response in the mosquito *Anopheles gambiae*. *Insect Mol Biol* 27:429–438
- Strader ME, Wong JM, Hofmann GE (2020) Ocean acidification promotes broad transcriptomic responses in marine metazoans: a literature survey. *Front Zool* 17:1–23
- Su W, Rong J, Zha S, Yan M, Fang J, Liu G (2018) Ocean acidification affects the cytoskeleton, lysozymes, and nitric oxide of hemocytes: a possible explanation for the hampered phagocytosis in blood clams. *Tegillarca Granosa Front Aquat Phys* 9:619. <https://doi.org/10.3389/fphys.2018.00619>
- Sunday JM, Calosi P, Dupont S, Munday PL, Stillman JH, Reusch TBH (2014) Evolution in an acidifying ocean. *Trends Ecol Evol* 29:117–125
- Suzuki M, Nagasawa H (2013) Mollusk shell structures and their formation mechanism. *Can J Zool* 91:349–366
- Talmage SC, Gobler CJ (2010) Effects of past, present, and future ocean carbon dioxide concentrations on the growth and survival of larval shellfish. *Proc Natl Acad Sci USA* 107:17246–17251. <https://doi.org/10.1073/pnas.0913804107>
- Tanio M, Kondo S, Sugio S, Kohno T (2007) Trivalent recognition unit of innate immunity system: crystal structure of trimeric human M-ficolin fibrinogen-like domain. *J Biol Chem* 282:3889–3895
- Thomsen J, Casties I, Pansch C, Körtzinger A, Melzner F (2013) Food availability outweighs ocean acidification effects in juvenile *Mytilus edulis*: laboratory and field experiments. *Glob Change Biol* 19:1017–1027
- Thomsen J, Haynert K, Wegner KM, Melzner F (2015) Impact of seawater carbonate chemistry on the calcification of marine bivalves. *Biogeosciences* 12:1543–1571. <https://doi.org/10.5194/bg-12-4209-2015>
- Thomsen J, Stapp LS, Haynert K, Schade H, Danelli M, Lanning G, Melzner F (2017) Naturally acidified habitat selects for ocean acidification-tolerant mussels. *Sci Adv* 3:e1602411. <https://doi.org/10.1126/sciadv.1602411>
- Todgham AE, Hofmann GE (2009) Transcriptomic response of sea urchin larvae *Strongylocentrotus purpuratus* to CO<sub>2</sub>-driven seawater acidification. *J Exp Biol* 212:2579–2594
- Tomanek L, Zuzow MJ, Ivanina AV, Beniash E, Sikolova IM (2011) Proteomic response to elevated pCO<sub>2</sub> level in eastern oysters, *Crassostrea virginica*: evidence for oxidative stress. *J Exp Biol* 214:1836–1844
- Timmins-Schiffman E, O'Donnell MJ, Friedman CS, Roberts SB (2013) Elevated pCO<sub>2</sub> causes developmental delay in early larval Pacific oysters, *Crassostrea gigas*. *Mar Biol* 160:1973–1982
- Timmins-Schiffman E, Coffey WD, Hua W, Nunn BL, Dickinson GH, Roberts SB (2014) Shotgun proteomics reveals physiological response to ocean acidification in *Crassostrea gigas*. *BMC Genomics* 15:951. <https://doi.org/10.1186/1471-2164-15-951>
- Trigg SA, Mitchell KR, Thompson RE, Eudeline B, Vadopalas B, Timmins-Schiffman EB, Roberts S (2020) Temporal proteomic profiling reveals insight into critical developmental processes and temperature-influenced physiological response differences in a bivalve mollusc. *BMC Genomics* 21:723. <https://doi.org/10.1101/2020.06.05.137059>
- Uthicke S, Deshpande NP, Liddy M, Patel F, Lamare M, Wilkins MR (2019) Little evidence of adaptation potential to ocean acidification in sea urchins living in “Future Ocean” conditions at a CO<sub>2</sub> vent. *Ecol Evol* 9:10004–100016
- Wage J, Lerebours A, Hardege JD, Rotchell JM (2016) Exposure to low pH induces molecular level changes in the marine worm, *Platynereis dumerilii*. *Ecotoxicol Environ Saf* 124:105–110
- Waldbusser GG, Salisbury JE (2014) Ocean acidification in the coastal zone from an organism's perspective: multiple system parameters, frequency domains, and habitats. *Ann Rev Mar Sci* 6:221–247
- Wallace RB, Baumann H, Great JS, Aller RC, Gobler CJ (2014) Coastal ocean acidification: the other eutrophication problem. *Estuar Coast Shelf Sci* 148:1–13
- Waldbusser GG, Brunner EL, Haley BA, Hales B, Langdon CJ, Prahlg FG (2013) A developmental and energetic basis linking larval oyster shell formation to acidification sensitivity. *Geophys Res Lett* 40(10):2171–2176. <https://doi.org/10.1002/grl.50449>
- Wang N, Lee YH, Lee J (2008) Recombinant perlucin nucleates the growth of calcium carbonate crystals: molecular cloning and characterization of perlucin from disk abalone, *Haliotis discus discus*. *Comp Biochem Physiol B: Biochem* 149:354–361. <https://doi.org/10.1016/j.cbpb.2007.10.007>
- Wang Q, Cao R, Ning X, You L, Mu C, Wang C, Wei L, Cong M, Wu H, Zhao J (2016) Effects of ocean acidification on immune response of the Pacific oyster *Crassostrea gigas*. *Fish and Shellfish Immunol* 49:24–33
- Wang X, Wang M, Wang W, Liu Z, Xu J, Jia Z, Chen H, Qiu L, Lv Z, Wang L, Song L (2020) Transcriptional changes of Pacific oyster *Crassostrea gigas* reveal essential role of calcium signal pathway in response to CO<sub>2</sub>-driven acidification. *Sci Total Environ* 741:140177. <https://doi.org/10.1015/j.scitotenv.2020.140177>
- Wei J, Liu B, Fan S, Li H, Chen M, Zhang B, Su J, Meng Z, Yu D (2017) Differentially expressed immune-related genes in hemocytes of the pearl oyster *Pinctada fucata* against allograft identified by transcriptome analysis. *Fish and Shellfish Immunol* 62:247–256
- Whitlock MC, Lotterhos KE (2015) Reliable detection of loci responsible for local adaptation: inference of a null model through trimming the distribution of F(ST). *Am Nat Supp* 1:S24–36
- Xiong Y, Hu L, Yan Z, Zhang J, Li H (2018) Transcriptomic analysis of embryo development in the invasive snail *Pomacea canaliculata*. *J Molluscan Stud* 84(3):233–239
- Yang B, Pu F, Li L, You W, Ke C, Feng D (2017) Functional analysis of a tyrosinase gene involved in early larval shell biogenesis in *Crassostrea angulata* and its response to ocean acidification. *Comp Biochem Physiol B Biochem Mol Biol* 206:8–15
- Zhang G, Fang X, Guo X, Li L, Luo R, Xu F, Wang J (2012a) The oyster genome reveals stress adaptation and complexity of shell formation. *Nature* 490:49–54. <https://doi.org/10.1038/nature11413>
- Zhang Z, Miteva MA, Wang L, Alexov E (2012b) Analyzing effects of naturally occurring missense mutations. *Comput Math Methods Med* 2012:805827. <https://doi.org/10.1155/2012/805827>
- Zhang G, Li L, Meng J, Qi H, Qu T, Xu F, Zhang L (2016) Molecular basis for adaptation of oysters to stressful marine intertidal environments. *Annu Rev Anim Bio* 4:357–381. <https://doi.org/10.1146/annurev-animal-022114-110903>
- Zhang C, Xue Z, Yu Z, Wang H, Liu Y, Li H, Song L (2020) A tandem-repeat galectin-1 from *Apostichopus japonicus* with broad

PAMP recognition pattern and antibacterial activity. *Fish Shellfish Immunol* 99:167–175

Zhao X, Shi W, Han Y, Liu S, Guo C, Fu W, Chai X, Liu G (2017) Ocean acidification adversely influences metabolism, extracellular pH and calcification of an economically important marine bivalve, *Tegillarca granosa*. *Mar Environ Res* 125:82–89

Zhao X, Han Y, Chen B, Xia B, Qu K, Liu G (2020) CO<sub>2</sub>-drive ocean acidification weakens mussel shell defense capacity and induces global molecular compensatory responses. *Chemosphere* 243:125415. <https://doi.org/10.1016/j.chemosphere.2019.125415>

**Publisher's Note** Springer Nature remains neutral with regard to jurisdictional claims in published maps and institutional affiliations.

Springer Nature or its licensor (e.g. a society or other partner) holds exclusive rights to this article under a publishing agreement with the author(s) or other rightsholder(s); author self-archiving of the accepted manuscript version of this article is solely governed by the terms of such publishing agreement and applicable law.